

NASA/CR-2010-216289



## **Peak Wind Tool for General Forecasting Phase II**

*Joe H. Barrett III*

*ENSCO, Inc., Cocoa Beach, Florida*

*NASA Applied Meteorology Unit, Kennedy Space Center, Florida*

---

**September 2010**

## NASA STI Program ... in Profile

Since its founding, NASA has been dedicated to the advancement of aeronautics and space science. The NASA scientific and technical information (STI) program plays a key part in helping NASA maintain this important role.

The NASA STI program operates under the auspices of the Agency Chief Information Officer. It collects, organizes, provides for archiving, and disseminates NASA's STI. The NASA STI program provides access to the NASA Aeronautics and Space Database and its public interface, the NASA Technical Report Server, thus providing one of the largest collections of aeronautical and space science STI in the world. Results are published in both non-NASA channels and by NASA in the NASA STI Report Series, which includes the following report types:

- **TECHNICAL PUBLICATION.** Reports of completed research or a major significant phase of research that present the results of NASA Programs and include extensive data or theoretical analysis. Includes compilations of significant scientific and technical data and information deemed to be of continuing reference value. NASA counterpart of peer-reviewed formal professional papers but has less stringent limitations on manuscript length and extent of graphic presentations.
- **TECHNICAL MEMORANDUM.** Scientific and technical findings that are preliminary or of specialized interest, e.g., quick release reports, working papers, and bibliographies that contain minimal annotation. Does not contain extensive analysis.
- **CONTRACTOR REPORT.** Scientific and technical findings by NASA-sponsored contractors and grantees.

- **CONFERENCE PUBLICATION.** Collected papers from scientific and technical conferences, symposia, seminars, or other meetings sponsored or co-sponsored by NASA.
- **SPECIAL PUBLICATION.** Scientific, technical, or historical information from NASA programs, projects, and missions, often concerned with subjects having substantial public interest.
- **TECHNICAL TRANSLATION.** English-language translations of foreign scientific and technical material pertinent to NASA's mission.

Specialized services also include organizing and publishing research results, distributing specialized research announcements and feeds, providing help desk and personal search support, and enabling data exchange services.

For more information about the NASA STI program, see the following:

- Access the NASA STI program home page at <http://www.sti.nasa.gov>
- E-mail your question via the Internet to [help@sti.nasa.gov](mailto:help@sti.nasa.gov)
- Fax your question to the NASA STI Help Desk at 443-757-5803
- Phone the NASA STI Help Desk at 443-757-5802
- Write to:  
NASA STI Help Desk  
NASA Center for Aerospace Information  
7115 Standard Drive  
Hanover, MD 21076-1320

NASA/CR-2010-216289



## Peak Wind Tool for General Forecasting Phase II

*Joe H. Barrett III*

*ENSCO, Inc., Cocoa Beach, Florida*

*NASA Applied Meteorology Unit, Kennedy Space Center, Florida*

National Aeronautics and  
Space Administration

*Kennedy Space Center  
Kennedy Space Center, FL 32899-0001*

---

**September 2010**

## **Acknowledgments**

The author thanks Mr. Mark Wheeler of the NASA Applied Meteorology Unit for providing expertise necessary to develop the MIDDS version of the tool. Personnel from the 45th Weather Squadron provided valuable feedback on the tool's user interface.

Available from:

NASA Center for AeroSpace Information  
7115 Standard Drive  
Hanover, MD 21076-1320  
443-757-5802

This report is also available in electronic form at

<http://science.ksc.nasa.gov/amu/>

## Executive Summary

The expected peak wind speed of the day is an important forecast element in the 45th Weather Squadron's (45 WS) daily 24-Hour and Weekly Planning Forecasts. The forecasts are used for ground and space launch operations at the Kennedy Space Center (KSC) and Cape Canaveral Air Force Station (CCAFS). The 45 WS also issues wind advisories for KSC/CCAFS when they expect wind gusts to meet or exceed 25 kt, 35 kt and 50 kt thresholds at any level from the surface to 300 ft. The 45 WS forecasters have indicated peak wind speeds are challenging to forecast, particularly in the cool season months of October - April. In Phase I of this task, the Applied Meteorology Unit (AMU) developed a tool to help the 45 WS forecast non-convective winds at KSC/CCAFS for the 24-hour period of 0800 to 0800 local time. The tool was delivered as a Microsoft Excel graphical user interface (GUI). The GUI displayed the forecast of peak wind speed, 5-minute average wind speed at the time of the peak wind, timing of the peak wind and probability the peak speed would meet or exceed 25 kt, 35 kt and 50 kt.

For the current task (Phase II), the 45 WS requested additional observations be used for the creation of the forecast equations by expanding the period of record (POR). Additional parameters were evaluated as predictors, including wind speeds between 500 ft and 3000 ft, static stability classification, Bulk Richardson Number, mixing depth, vertical wind shear, temperature inversion strength and depth and wind direction. Using a verification data set, the AMU compared the performance of the Phase I and II prediction methods. Just as in Phase I, the tool was delivered as a Microsoft Excel GUI. The 45 WS requested the tool also be available in the Meteorological Interactive Data Display System (MIDDS).

The AMU first expanded the POR by two years by adding tower observations, surface observations and CCAFS (XMR) soundings for the cool season months of March 2007 to April 2009. The POR was expanded again by six years, from October 1996 to April 2002, by interpolating 1000-ft sounding data to 100-ft increments. The Phase II developmental data set included observations for the cool season months of October 1996 to February 2007. The AMU calculated 68 candidate predictors from the XMR soundings, to include 19 stability parameters, 48 wind speed parameters and one wind shear parameter. Each day in the data set was stratified by synoptic weather pattern, low-level wind direction, precipitation and Richardson Number, for a total of 60 stratification methods. Linear regression equations, using the 68 predictors and 60 stratification methods, were created for the tool's three forecast parameters: the highest peak wind speed of the day (PWSD), 5-minute average speed at the same time (AWSD), and timing of the PWSD. For PWSD and AWSD, 30 Phase II methods were selected for evaluation in the verification data set. For timing of the PWSD, 12 Phase II methods were selected for evaluation.

The verification data set contained observations for the cool season months of March 2007 to April 2009. The data set was used to compare the Phase I and II forecast methods to climatology, model forecast winds and wind advisories issued by the 45 WS. The model forecast winds were derived from the 0000 and 1200 UTC runs of the 12-km North American Mesoscale (MesoNAM) model. The forecast methods that performed the best in the verification data set were selected for the Phase II version of the tool. For PWSD and AWSD, linear regression equations based on MesoNAM forecasts performed significantly better than the Phase I and II methods. For timing of the PWSD, none of the methods performed significantly better than climatology.

The AMU then developed the Microsoft Excel and MIDDS GUIs. The GUIs display the forecasts for PWSD, AWSD and the probability the PWSD will meet or exceed 25 kt, 35 kt and 50 kt. Since none of the prediction methods for timing of the PWSD performed significantly better than climatology, the tool no longer displays this predictand. The Excel and MIDDS GUIs display forecasts for Day-1 to Day-3 and Day-1 to Day-5, respectively. The Excel GUI uses MesoNAM forecasts as input, while the MIDDS GUI uses input from the MesoNAM and Global Forecast System model. Based on feedback from the 45 WS, the AMU added the daily average wind speed from 30 ft to 60 ft to the tool, which is one of the parameters in the 24-Hour and Weekly Planning Forecasts issued by the 45 WS. In addition, the AMU expanded the MIDDS GUI to include forecasts out to Day-7.

## Table of Contents

Executive Summary .....	1
1 Introduction .....	7
2 Data.....	8
2.1 Tower Data.....	8
2.2 Surface Observations .....	9
2.3 Sounding Data.....	9
3 Development of Phase II Prediction Equations .....	14
3.1 Synoptic Weather Pattern.....	14
3.2 Phase II Predictors .....	14
3.3 Prediction Equations for PWSD and AWSD .....	18
3.4 Timing of PWSD .....	20
4 Independent Verification of Prediction Methods.....	22
4.1 Peak and Average Wind Speed.....	27
4.1.1 <i>Comparing Phase I and II Methods to Climatology</i> .....	27
4.1.2 <i>Comparing Phase I and II Methods to Model Forecast Winds</i> .....	31
4.1.3 <i>Comparison of Phase I and II Peak Wind Speed Predictions to 45 WS Wind Advisories</i> .....	35
4.2 Timing of the Peak Wind .....	35
5 Peak Wind Tool GUIs .....	38
5.1 Microsoft Excel GUI.....	38
5.1.1 <i>Equation Development</i> .....	38
5.1.2 <i>Using the Excel GUI</i> .....	42
5.2 MIDDS GUI.....	45
5.2.1 <i>Equation Development</i> .....	46
5.2.2 <i>Point Model Data</i> .....	47
5.2.3 <i>Using the MIDDS GUI</i> .....	47
6 Summary and Future Work .....	49
6.1 Summary .....	49
6.2 Future Work .....	50
References.....	51
List of Acronyms .....	52

## List of Figures

Figure 1.	A map showing the towers used in the task. Except for tower 0300 (lower-right, in blue), only the yellow- and red-colored towers were used.....	9
Figure 2.	Comparison of 100-ft sounding data on 1 January 2003 to interpolated data using Method 1 (left) and Method 2 (right). .....	10
Figure 3.	Monthly averages of height versus u-wind component, using interpolated (dashed) and 100-ft data (solid). The interpolated data used Method 1 (left) and Method 2 (right). The data are from the cool season months in the period October 2002 – April 2008. ....	11
Figure 4.	Monthly averages of height versus MAE in u-wind component, using interpolated and 100-ft data. The data were interpolated using Method 1 (left) and Method 2 (right). .....	11
Figure 5.	The December plots of height versus MAE in u-wind component, using interpolated and 100-ft data. The data were interpolated using Method 1 (left) and Method 2 (right). The 2002-2007 December average is displayed by the black lines. ....	12
Figure 6.	Height versus MAE in u- (left) and v-wind (right) components, using Method 1 (red) and Method 2 (green) interpolated data. The interpolated data were averaged over all months in the POR. ....	12
Figure 7.	Height versus MAE in temperature (left) and dew point (right), using Method 1 (red) and Method 2 (green) interpolated data. The interpolated data were averaged over all months in the POR. ....	13
Figure 8.	MAE values for least-squares single linear regression equations for PWSD (left) and AWSD (right). The MAE is shown for the stability parameters (S1-S19), wind speed parameters (W1-W48) and wind shear parameter (H1). Mean MAE (blue) is the average of all stratification methods, while Minimum MAE (red) is the lowest of all stratification categories. ....	18
Figure 9.	MAE values for robust single linear regression equations for PWSD (left) and AWSD (right). The MAE is shown for the stability parameters (S1-S19), wind speed parameters (W1-W48) and wind shear parameter (H1). Mean MAE (blue) is the average of all stratification categories, while Minimum MAE (red) is the lowest of all stratification categories.....	18
Figure 10.	Mean MAE values for least-squares (blue) and robust (red) single linear regression equations for PWSD (left) and AWSD (right). The MAE is shown for the 60 stratifications (x-axis)...	19
Figure 11.	Mean MAE values for least-squares (blue), robust (red) and least-trimmed squares (green) multiple linear regression equations for PWSD (left) and AWSD (right). The MAE is shown for the 60 stratifications (x-axis). ....	20
Figure 12.	MAE values for least-squares (left) and robust (right) single linear regression equations for timing of the PWSD. The values are shown for the stability parameters (S1-S19), wind speed parameters (W1-W48) and wind shear parameter (H1). Mean MAE (blue) is the average of all stratification methods. Minimum MAE (red) is the lowest of all stratification categories.20	
Figure 13.	Mean MAE values for single (left) and multiple (right) linear regression equations for timing of the peak wind. The least squares and robust regressions are in blue and red, while the least-trimmed regressions are in green. The values are shown for the 60 stratifications (x-axis). ..	21
Figure 14.	Mean Error for PWSD (left) and AWSD (right) on non-precipitation days For the Phase II methods, points 1-6 (on x-axis) correspond to stratification methods SM1-SM6, respectively. The legend describes the colors corresponding to the Phase II linear regression types. Refer to	

	Table 3 for a description of the stratification methods and linear regression types. The climatology methods are plotted on points 1-4. The Phase I method is plotted on point 1. ...	27
Figure 15.	Mean Error for PWSD (left) and AWS D (right) on precipitation days, for the climatology and Phase I and II methods. Refer to Figure 14 for a description of the x-axis. ....	28
Figure 16.	MAE for PWSD (left) and AWS D (right) on non-precipitation days, for the climatology and Phase I and II methods. Refer to Figure 14 for a description of the x-axis. ....	28
Figure 17.	MAE for PWSD (left) and AWS D (right) on precipitation days, for the climatology and Phase I and II methods. Refer to Figure 14 for a description of the x-axis. ....	29
Figure 18.	Mean Error for PWSD on days in which the forecast's absolute error is within 5 kt (left) and greater than 5 kt (right). Refer to Figure 14 for a description of the x-axis. ....	30
Figure 19.	Mean Error for AWS D on days in which the forecast's absolute error is within 5 kt (left) and greater than 5 kt (right). Refer to Figure 14 for a description of the x-axis. ....	30
Figure 20.	Average difference between the PWSD and the tower-average peak speed, on days in which the forecast's absolute error is within 5 kt (left) and greater than 5 kt (right). Refer to Figure 14 for a description of the x-axis. ....	31
Figure 21.	Mean Error for PWSD and AWS D. The strongest 24-hour 0000 UTC MesoNAM forecast winds are plotted on points 1-20, in black. The 0000 UTC MesoNAM linear regression forecasts are plotted on points 1-20, in light blue. The climatology methods are plotted on points 1-4, in dark blue. The Phase I method is plotted on point 1 (in red), and the Phase II methods are plotted on points 1-30 (in yellow). Refer to Table 3 for a description of the Phase II methods .....	32
Figure 22.	MAE for PWSD and AWS D. Refer to Figure 21 for a description of the x-axis. ....	33
Figure 23.	Mean Error for PWSD on precipitation (left) and non-precipitation days (right). Refer to Figure 21 for a description of the x-axis. ....	33
Figure 24.	Mean Error for AWS D on precipitation (left) and non-precipitation days (right). Refer to Figure 21 for a description of the x-axis. ....	33
Figure 25.	MAE for PWSD on precipitation (left) and non-precipitation days (right). Refer to Figure 21 for a description of the x-axis. ....	34
Figure 26.	MAE for AWS D on precipitation (left) and non-precipitation days (right). Refer to Figure 21 for a description of the data points. ....	34
Figure 27.	MAE for PWSD (left) and AWS D (right), for 0000 and 1200 UTC MesoNAM regression forecasts. Points 1-17 depict model levels 2-18, and points 18-20 depict the strongest winds in the lowest 1000-, 2000-, and 3000-ft of the model. The legend shows the color corresponding to each method. ....	34
Figure 28.	Mean Error (diamonds) and MAE (circles) for timing of the peak wind. The Phase I method is plotted on point 1, Phase II methods on points 1-12, climatology methods on points 1-4 and 0000 UTC MesoNAM winds on points 1-20. ....	37
Figure 29.	The Mean Error (diamonds) and MAE (triangles) for the timing of the peak wind by the 0000 and 1200 UTC MesoNAM winds. ....	37
Figure 30.	MAE for PWSD on precipitation (left) and non-precipitation (right) days, for Day-1 to Day-3 forecasts. Forecasts are from linear regression equations using the 0000 UTC MesoNAM forecast winds. Points 1-17 depict model levels 2-18, and points 18-20 depict the strongest winds in the lowest 1000-, 2000- and 3000-ft of the model. ....	39

Figure 31.	MAE for PWSd on precipitation (left) and non-precipitation (right) days, for Day-1 to Day-3 forecasts. Forecasts are from linear regression equations using the 1200 UTC MesoNAM forecast winds. Points 1-17 depict model levels 2-18, and points 18-20 depict the strongest winds in the lowest 1000-, 2000- and 3000-ft of the model.....	39
Figure 32.	MAE for AWSd on precipitation (left) and non-precipitation (right) days, for Day-1 to Day-3 forecasts. Forecasts are from linear regression equations using the 0000 UTC MesoNAM forecast winds. Points 1-17 depict model levels 2-18, and points 18-20 depict the strongest winds in the lowest 1000-, 2000- and 3000-ft of the model.....	40
Figure 33.	MAE for AWSd on precipitation (left) and non-precipitation (right) days, for Day-1 to Day-3 forecasts. Forecasts are from linear regression equations using the 1200 UTC MesoNAM forecast winds. Points 1-17 depict model levels 2-18, and points 18-20 depict the strongest winds in the lowest 1000-, 2000- and 3000-ft of the model.....	40
Figure 34.	Intro worksheet to start the Excel version of the Peak Wind Tool.....	42
Figure 35.	Dialog box used to select a MesoNAM input file.....	43
Figure 36.	Dialog box used to select the forecast day.....	44
Figure 37.	GUI displaying the output from the Excel version of the Peak Wind tool. The top section shows the predicted PWSd, the middle section shows the predicted AWSd, and the bottom section shows the probability the PWSd will meet or exceed 25 kt, 35 kt and 50 kt.....	45
Figure 38.	MAE for daily average speed for forecasts from 0000 (left) and 1200 UTC (right) MesoNAM. Forecasts for precipitation days are plotted on points 1, 4 and 7 of the x-axis. Forecasts for non-precipitation days are plotted on points 2, 5 and 8, and forecasts for all days are plotted on points 3, 6 and 9. ....	47
Figure 39.	MIDDS version of the Peak Wind Tool showing forecasts from the 7 July 2010 model runs. Forecasts for precipitation days have the header "Precip", while non-precipitation days have the header "NoPrecip". The header "All" includes days with and without precipitation. ....	48

## List of Tables

Table 1. ....	16
Table 2. ....	17
Table 3. Phase II methods verified for PWSD, AWSD and timing of the PWSD. Methods in red were not verified for the timing of the PWSD. ....	23
Table 4. Stratification categories used in Phase II methods. Wind direction was based on the vector average wind in the lowest 300 ft of XMR sounding. The stratification methods are described in Table 3. ....	24
Table 5. Stratification category and predictors for each PWSD equation using single linear regression. The stratification categories are described in Table 4. ....	25
Table 6. Stratification category and predictors for each PWSD equation using multiple linear regression. The stratification categories are described in Table 4. ....	26
Table 7. Average heights and standard deviations of the MesoNAM vertical levels used in the verification data. ....	32
Table 8. Verification for days in which the highest 45 WS wind warning/advisory was 25-34 kt (left) and 35-49 kt (right). Phase II methods are shown in blue. ....	35
Table 9. Climatology methods for predicting timing of the peak wind, based on the mean peak winds in a previous AMU task (Lambert 2002). The “average wind speed” is the average of all the towers used in the previous AMU task, and the “maximum wind speed” is the maximum of all the towers. ....	36
Table 10. Prediction equations for PWSD, based on linear regressions in which the predictor is the strongest 24-hour wind speed at the MesoNAM model level, and the predictand is the PWSD. Refer to Table 7 for the height of each model level. ....	41
Table 11. Prediction equations for AWSD, based on linear regressions in which the predictor is the strongest 24-hour wind speed at the MesoNAM model level, and the predictand is the AWSD. Refer to Table 7 for the height of each model level. ....	41
Table 12. MAE (kt) for daily average speed. “All Days” is all days in the verification data set. “W. Avg” is the weighted average of precipitation and non-precipitation days. “00 UTC” is the 0000 UTC MesoNAM and “12 UTC” is the 1200 UTC MesoNAM. ....	47

## 1 Introduction

The expected peak wind speed of the day is an important element in the 45th Weather Squadron's (45 WS) daily 24-Hour and Weekly Planning Forecasts. The forecasts are used for ground and space launch operations at the Kennedy Space Center (KSC) and Cape Canaveral Air Force Station (CCAFS). The 24-Hour Forecast is valid from 0800 to 0800 local time the next day, and it is broken into six 4-hour time blocks. The Weekly Forecast is for the next six days starting with the next day and is divided into 12-hour time blocks. The 45 WS also issues wind advisories for KSC/CCAFS and Patrick Air Force Base (PAFB) when they expect peak gusts to meet or exceed 25 kt, 35 kt and 50 kt thresholds at any level from the surface to 300 ft.

The 45 WS forecasters have indicated peak wind speeds are challenging to forecast, particularly in the cool season months of October – April. In Phase I of this task (Barrett and Short 2008), the Applied Meteorology Unit (AMU) developed a tool to help them forecast non-convective winds during the cool season for the 24-Hour Forecast. The tool forecasts the highest peak wind speed, the timing of the peak speed and the 5-minute average wind speed at the time of the peak wind from the surface to 300 ft on KSC/CCAFS. In addition, it provides the probability the peak speed will meet or exceed the wind advisory thresholds. The tool calculates its forecasts based on the morning CCAFS sounding (XMR), the synoptic weather pattern and whether or not precipitation is expected over KSC/CCAFS during the 24-hour period.

For Phase II, the 45 WS requested additional observations be used in the creation of the forecast equations by expanding the period of record (POR). Additional parameters were evaluated, including wind speeds between 500 ft and 3000 ft, static stability classification, Bulk Richardson Number, mixing depth, vertical wind shear, inversion strength and depth and wind direction. Using a verification data set, the AMU compared the Phase I and II prediction methods to climatology and model forecasts. The methods that performed the best in the verification data set were selected for the Phase II tool. As in Phase I, the tool was delivered as a Microsoft Excel graphical user interface (GUI). The 45 WS requested the AMU also make the tool available in the Meteorological Interactive Data Display System (MIDDS), their main weather display system, to provide the ability to produce 5-day forecasts quickly.

## 2 Data

In Phase I and Phase II, three types of observations were used: 5-minute observations from the KSC/CCAFS tower network, hourly and special surface observations from the Shuttle Landing Facility (SLF) and XMR soundings. The tower observations and soundings were obtained from the Range Technical Services Contractor, Computer Sciences Raytheon (CSR). Surface observations were obtained from the 14th Weather Squadron Strategic Climatic Information Service. In Phase I, the data set included observations from the cool season months of October 2002 to February 2007. In Phase II, cool season data from March 2007 to April 2009 were added to the existing data set. Days in which east-central Florida was under the influence of a tropical cyclone were removed from the data set, since only cool-season weather phenomena were of interest.

The prediction equations in the Phase I tool required sounding data in 100-ft increments. To increase the size of the Phase II data set even further, the AMU evaluated whether data prior to October 2002 could be added by interpolating 1000-ft sounding data down to 100-ft increments. Sounding data between October 1996 and April 2002 are only available in 1000-ft increments, while data between October 2002 and April 2009 are available in both 1000-ft and 100-ft increments. The AMU interpolated the 1000-ft data from October 1996 to April 2008 to 100-ft increments, and then compared the interpolated data to the 100-ft data for the period October 2002 to April 2008. Since no significant differences were found between the interpolated and 100-ft data, the interpolated data from October 1996 to April 2002 were included in the Phase II data set. The 100-ft data were used for the period October 2002 to April 2009.

The tool predicts the peak wind in the 24-hour period 0800 to 0800 local time. The tool's prediction equations used observations from the 24-hour period 1300 to 1300 UTC, since the majority of days in the cool season were in Eastern Standard Time (EST).

### 2.1 Tower Data

Data were collected from all 32 towers used to verify wind advisories issued by the 45 WS. Their locations are shown in Figure 1. Tower 0300, which is not used to verify wind advisories, was also used in order to provide better coverage of the southern portion of KSC. The meteorological variables in the tower data set included temperature and relative humidity, 5-minute average and peak wind speeds, 5-minute average and peak wind directions, and the standard deviation of the 5-minute average wind direction over a 30-minute period. Wind speed and direction data were sampled every second. The peak wind was the maximum 1-second speed in the 5-minute period. Case and Bauman (2004) provides a detailed description of the KSC/CCAFS tower network instrumentation. Since 45 WS wind advisories apply to winds up to 300 ft, only tower wind observations up to 300 ft were used in this task.

Lambert (2002) describes the automated quality control (QC) algorithms and associated Fortran software to flag bad tower data prior to analysis. The AMU rewrote the QC software in the Java programming language to make it more portable and easier to maintain. For example, Java software does not need to be recompiled in order to run on multiple computer operating systems. The Java version uses a configuration text file to store values previously hard-coded in the software, such as the years in the POR and the list of wind tower identifiers. This allows the user to easily change the parameters by modifying the configuration file. Previously, the user had to edit the source code and recompile the software. The AMU also fixed a bug in the Fortran software, which did not properly handle the case in which a sensor's height changed during the POR. In addition, a supplementary QC algorithm was added to check for repeating observations that can occur during a sensor outage.

After the QC software was run, the peak wind speed of the day (PWSD) was determined from the 33 towers at all levels up to 300 ft. The 5-minute average wind speed at the tower reporting the PWSD was also recorded. The AMU manually examined each PWSD of 60 kt or greater to check for erroneous outliers. If the observations from the tower appeared erroneous, then the highest daily peak wind speed from one of the other towers was used.

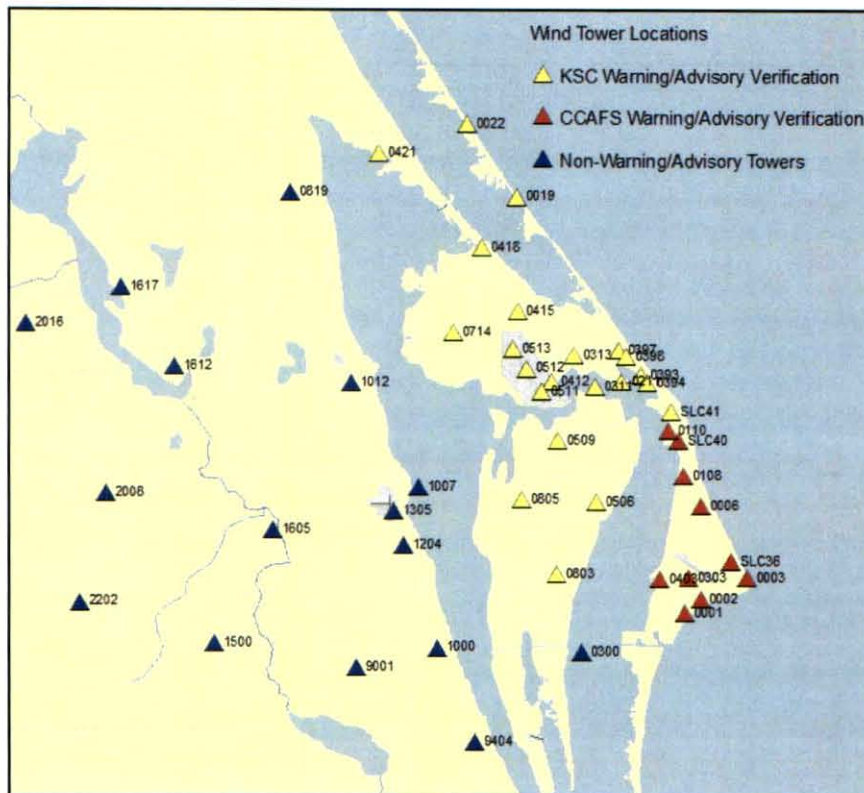


Figure 1. A map showing the towers used in the task. Except for tower 0300 (lower-right, in blue), only the yellow- and red-colored towers were used.

## 2.2 Surface Observations

The SLF hourly and special observations were used to determine if precipitation occurred at or within 5 NM (the vicinity) of the SLF at least once during each 24-hour period. Each day was then classified as a precipitation- or non-precipitation day.

## 2.3 Sounding Data

The XMR soundings were used to create the candidate predictors for PWSD, timing of the PWSD and the 5-minute average wind at the time of the PWSD (hereafter referred to as AWSD). The soundings included wind speed and direction, pressure, temperature and dew point. Only soundings between 0930 UTC and 1230 UTC were used, since soundings outside this time period may be unrepresentative due to diurnal changes in temperature, humidity and wind. If a sounding did not extend to at least 15,000 ft mean sea level (MSL), the sounding was eliminated from the data set. If there were multiple soundings between 0930 UTC and 1230 UTC, the latest one was used.

All of the sounding data needed to be in 100-ft increments to calculate the predictors. While data from October 2002 to April 2009 were already available in 100-ft increments, data between October 1996 and April 2002 were only available in 1000-ft increments. If the 1000-ft sounding data could be interpolated to 100-ft increments without a significant loss in accuracy, the interpolated sounding data would be used in the Phase II data set.

The 1000-ft sounding data from October 1996 to April 2008 were interpolated to 100-ft increments up to 15,000 ft MSL, using two different methods. In Method 1, data at the 1000-ft, significant and

mandatory levels were linearly interpolated to 100-ft increments. In Method 2, only the significant and mandatory level data were linearly interpolated to 100-ft increments. A significant level occurs when there is a significant change in temperature or wind with height. Therefore, the number and heights of the significant levels were variable. Up through 15,000 ft MSL, mandatory levels in the XMR soundings were at 1000 mb, 950 mb, 900 mb, 850 mb, 800 mb, 750 mb, 700 mb, 650 mb and 600 mb. In July 2002, another mandatory level was added at 925 mb.

The AMU compared the interpolated data to the 100-ft sounding data for the period October 2002 to April 2008. First, the AMU compared individual soundings from a small sample of seven days in the 2002/2003 cool season (October 2002 to April 2003). As an example, Figure 2 compares the 100-ft data in the 1 January 2003 XMR sounding to the interpolated data using Method 1 and 2. The Method 1 and 2 wind speeds are nearly identical, except around 6000 ft MSL. The following conclusions were reached after analyzing data from the seven soundings:

- The 100-ft data were usually similar to the interpolated data,
- The interpolated data were usually closer to each other than to the 100-ft data,
- The differences between the Method 1 and Method 2 interpolated data were largest at multiples of 1000 ft MSL,
- At multiples of 1000 ft MSL, the Method 1 interpolated and 100-ft data were usually exactly the same, especially for temperature, dew point, and relative humidity,
- Due to the high vertical variability in dew point, there were occasionally large (on the order of 5 °C) differences between the interpolated and 100-ft data, and
- There were occasionally large differences between the interpolated and 100-ft data in wind speed and direction (on the order of 5 kt and 90°).

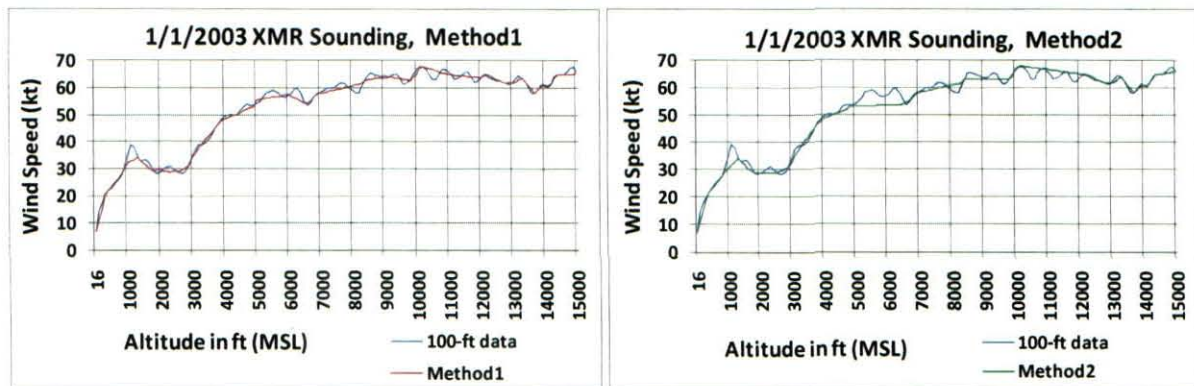


Figure 2. Comparison of 100-ft sounding data on 1 January 2003 to interpolated data using Method 1 (left) and Method 2 (right).

Next, the monthly averages for the interpolated and 100-ft data were compared for the cool season months in the period October 2002 to April 2008. The averages were practically equal for each month, indicating no significant biases in the interpolated data. As an example, Figure 3 compares the u-wind component in the 100-ft and interpolated data for each month. The figure shows no significant differences between the interpolated (dashed lines) and 100-ft (solid lines) data in the monthly averages.

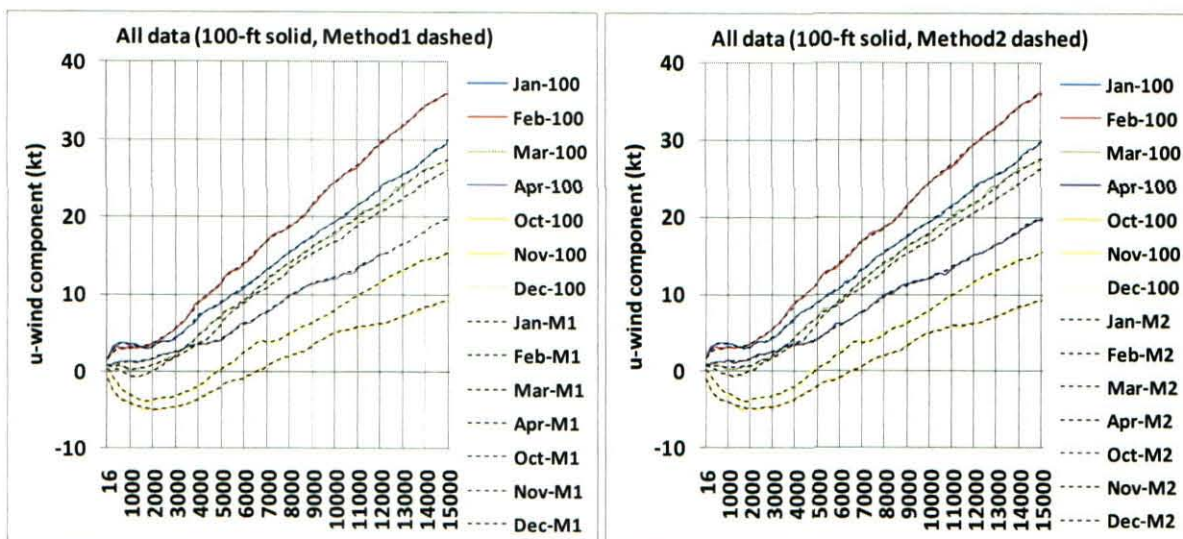


Figure 3. Monthly averages of height versus u-wind component, using interpolated (dashed) and 100-ft data (solid). The interpolated data used Method 1 (left) and Method 2 (right). The data are from the cool season months in the period October 2002 – April 2008.

The AMU compared the interpolated and 100-ft data using mean absolute error (MAE). The MAE is the mean of the absolute value of the differences between the interpolated and 100-ft data. The MAE monthly averages for wind varied by height, but were generally between 0.5 and 1.0 kt. As an example, Figure 4 shows the MAE monthly averages of the u-wind component versus height. The figure shows very little scatter in the monthly averages, and the MAE of the Method 1 data was smaller than the Method 2 data. The MAE minimums correlated to the mandatory pressure levels. There were also secondary MAE minimums for Method 1 at multiples of 1000-ft MSL. While the monthly averages of MAE contained little scatter, MAE for individual months had more scatter. For example, Figure 5 shows a fairly large amount of scatter in the MAE for the u-wind component in December.

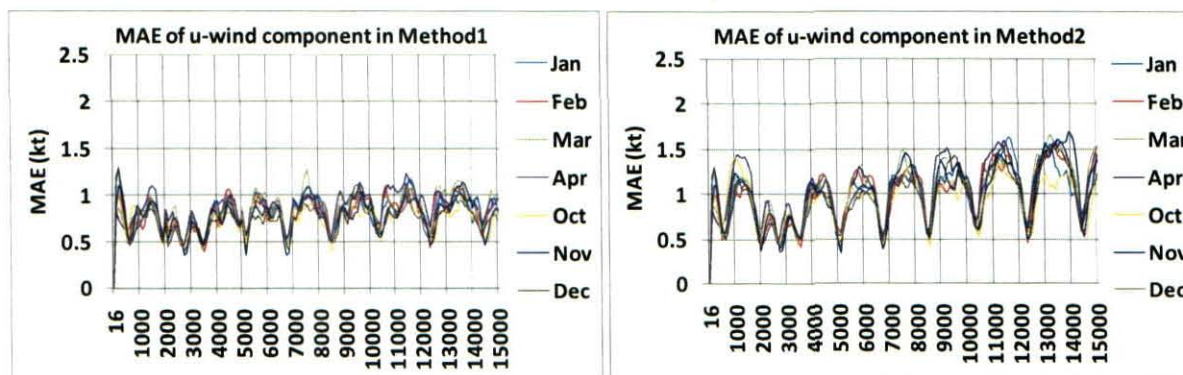


Figure 4. Monthly averages of height versus MAE in u-wind component, using interpolated and 100-ft data. The data were interpolated using Method 1 (left) and Method 2 (right).

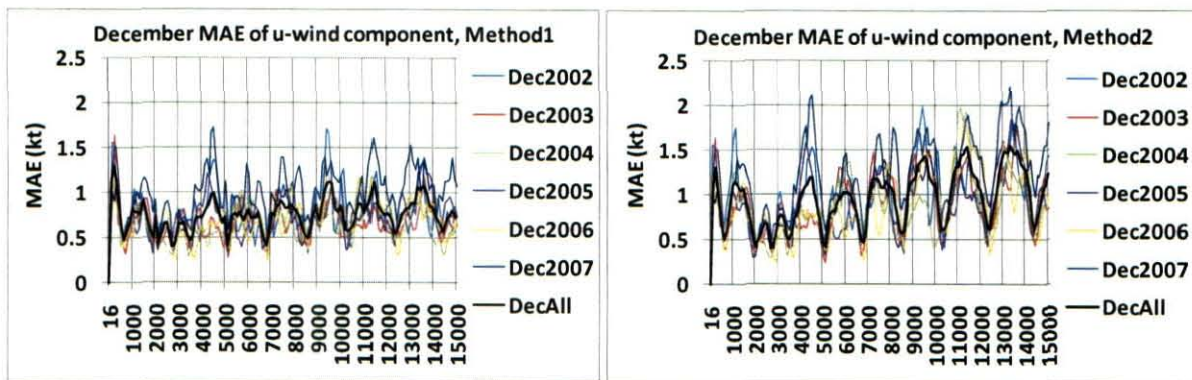


Figure 5. The December plots of height versus MAE in u-wind component, using interpolated and 100-ft data. The data were interpolated using Method 1 (left) and Method 2 (right). The 2002-2007 December average is displayed by the black lines.

When averaging the MAE over the cool-season months from 2002 to 2008, comparing the MAE of Method 1 and 2 showed a clearer pattern. Figure 6 compares the MAE of the u- and v-wind components using the Method 1 and 2 interpolated data. The MAE pattern was practically the same between the u-wind (left) and v-wind (right) components, and the MAE of Method 1 was lower than Method 2. At the mandatory levels the MAE was the same in the two interpolation methods, which was expected since both methods used mandatory level data. The difference in MAE between the two methods was maximized near multiples of 1000-ft MSL, unless a mandatory level happened to be nearby.

Figure 7 compares the MAE of the temperature and dew point data. Method 1 had the lowest MAE for temperature and dew point. The MAE values were small for Method 1 and 2, on the order of 0.1 °C and 0.2-0.6 °C for temperature and dew point, respectively.

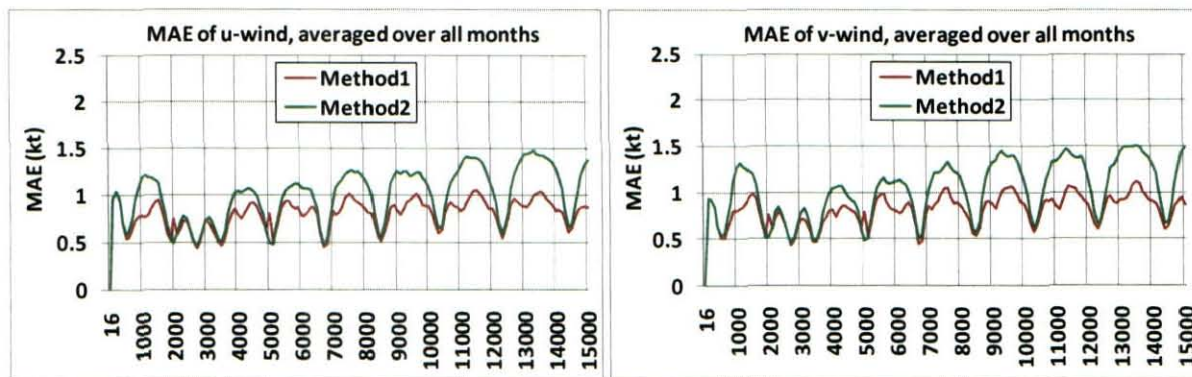


Figure 6. Height versus MAE in u- (left) and v-wind (right) components, using Method 1 (red) and Method 2 (green) interpolated data. The interpolated data were averaged over all months in the POR.

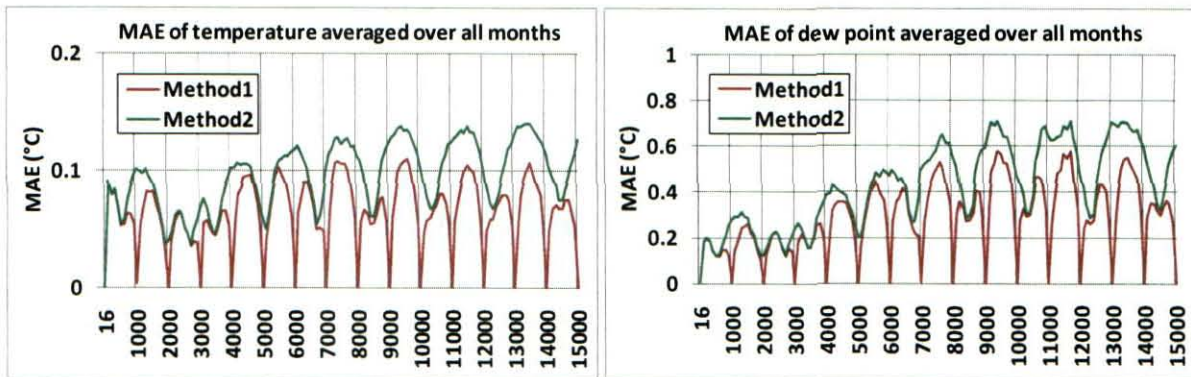


Figure 7. Height versus MAE in temperature (left) and dew point (right), using Method 1 (red) and Method 2 (green) interpolated data. The interpolated data were averaged over all months in the POR.

For temperature and dew point, the MAE of Method 1 was near 0 °C at multiples of 1000 ft MSL. On the other hand, for u- and v-wind components, the MAE of Method 1 was between 0.5 and 1.0 kt at multiples of 1000 ft MSL. The AMU investigated the reasoning behind this. According to CSR staff, the 1000-ft winds are smoothed by averaging over a 1000-ft interval (Mr. Rick Kulow of CSR, personal communication). For example, the 3000 ft wind is derived by smoothing the raw wind data from 2500 ft to 3500 ft. The other meteorological variables, such as temperature or dew point, are not smoothed in the 1000-ft data. For all of the meteorological variables, raw data (i.e. not smoothed) are used for the mandatory, significant and 100-ft data.

The AMU made the following conclusions after analyzing the monthly averages of MAE for the interpolated data:

- For all of the meteorological variables except pressure, a minimum in MAE occurred at the mandatory levels and a maximum in MAE occurred halfway between mandatory levels,
- A secondary minimum in MAE occurred in the Method 1 interpolated data at multiples of 1000 ft MSL,
- For pressure, the maximum in MAE occurred at mandatory levels and the minimum occurred halfway between the mandatory levels, and
- For all meteorological variables, the Method 1 interpolated data's MAE was lower than the Method 2 interpolated data.

Since no significant differences were found between the interpolated and 100-ft sounding data, the AMU used interpolated sounding data for the October 1996 to April 2002 period and 100-ft data for the October 2002 to April 2009 period. Method 1 was used to interpolate the sounding data since it had the lowest MAE values.

### 3 Development of Phase II Prediction Equations

The QC'd observation data were used to develop prediction equations for each forecast parameter. The developmental data set, consisting of cool-season observations from October 1996 to February 2007, was used to develop the prediction equations. The verification data set, containing cool-season observations from March 2007 to April 2009, was later used to independently verify the performance of the Phase II equations.

#### 3.1 Synoptic Weather Pattern

The AMU stratified each day in the data set by synoptic weather pattern to develop separate prediction equations for each weather pattern. The surface synoptic weather pattern at 1200 UTC was analyzed for each day using surface charts obtained from the National Weather Service (NWS) Hydrometeorological Prediction Center's short-term and long-term archives ([http://docs.lib.noaa.gov/rescue/dwm/data\\_rescue\\_daily\\_weather\\_maps.html](http://docs.lib.noaa.gov/rescue/dwm/data_rescue_daily_weather_maps.html)). Each day was categorized into one of the following:

- High pressure over Florida, with light and variable winds across east-central Florida,
- High pressure to the north or west of central Florida, with northwest, north, northeast, or east winds across east-central Florida,
- High pressure to the south or east of central Florida, with southeast, south, southwest, or west winds across east-central Florida,
- Cold front over north Florida,
- Cold or stationary front over central Florida,
- Cold or stationary front over south Florida or Florida Keys,
- Tropical storm or hurricane affecting Florida, and
- Surface weather map unavailable.

Only one day had a missing surface weather map. The days in which a tropical storm or hurricane affected Florida were removed from the data set to make the analysis more representative of the cool season.

#### 3.2 Phase II Predictors

The AMU wrote and executed Perl scripts to calculate the candidate predictors from the XMR soundings. The predictors were evaluated for their skill in predicting the PWSD, AWSD and timing of the PWSD. The predictors included 68 wind shear, stability and wind speed parameters. There were 19 stability parameters (identifiers in parentheses):

- Temperature inversion depth and strength (S1 - S2),
- Differences in temperature between 1000 ft and 16, 100, 200, 300, 400 and 500 ft (S3 - S8),
- Differences in temperature between 2000 ft and 16, 100, 200, 300, 400 and 500 ft (S9 - S14),
- Afternoon mixing height (S15 - S17), and
- Gradient Richardson Number (S18 - S19).

There were 48 wind speed parameters:

- Maximum wind speeds from the surface to 500 ft, 1000 ft, 2000 ft and 3000 ft (W1 - W4),
- Maximum wind speed between 1000 ft and 2000 ft (W5),
- Maximum wind speed between 2000 ft and 3000 ft (W6),
- Average wind speed from the surface to 500 ft and 1000 ft (W7 - W8),

- Average wind speed between 500 ft and 1000 ft (W9),
- Average wind speed between 1000 ft and 2000 ft (W10),
- Average wind speed between 2000 ft and 3000 ft (W11),
- Wind speeds at 16 ft through 3000 ft, by 100-ft increments (W12 - W42),
- Wind speed at the afternoon mixing height (W43 - W45), and
- Maximum wind speed from the surface to afternoon mixing height (W46 - W48).

There was one wind shear parameter: wind shear between the surface and 1000 ft (H1). Table 1 describes the stability and wind shear parameters, while Table 2 describes the wind speed parameters.

Table 1. Stability and wind shear parameters calculated from XMR soundings. Heights in MSL.	
<i>Parameter name</i>	<i>Description</i>
<b>inv.depth (S1)</b>	Depth of the surface-based inversion in ft. The top of the inversion was defined as the first level in which the temperature did not increase with height.
<b>inv.str.C (S2)</b>	Strength of the surface-based inversion in °C, defined as the difference between the temperatures at the surface and top of the inversion.
<b>X16...1000 to X500...1000 (S3 - S8)</b>	The difference between the temperature (°C) at 16 ft (or 100 ft, 200 ft, 300 ft, 400 ft, and 500 ft) and 1000 ft.
<b>X16...2000 to X500...2000 (S9 - S14)</b>	The difference between the temperature (°C) at 16 ft (or 100 ft, 200 ft, 300 ft, 400 ft, and 500 ft) and 2000 ft.
<b>mixhgtL1 (S15)</b>	Morning mixing height (in ft), defined as the height at which the temperature lapse rate first meets or exceeds 4 °C/km. This was based on an average saturated adiabatic lapse rate of 4-5 °C/km near the surface in temperature above freezing ( <a href="http://en.wikipedia.org/wiki/Lapse_rate">http://en.wikipedia.org/wiki/Lapse_rate</a> ).
<b>mixhgtL2 (S16)</b>	Morning mixing height (in ft) calculated by the same method as <b>mixhgtL1</b> , except data was in 200-ft increments instead of 100-ft.
<b>mixhgtT (S17)</b>	Afternoon mixing height based on the forecast maximum temperature, in ft. The forecast maximum was derived by adding 2 degrees Kelvin to the average boundary-layer potential temperature.
<b>br1 (S18)</b>	Bulk Richardson Number (BRN) for the lowest 1000 ft in the sounding. The BRN was calculated by averaging the gradient Richardson number between the surface and 1000 ft ( <a href="http://amsglossary.allenpress.com/glossary/search?id=bulk-richardson-number1">http://amsglossary.allenpress.com/glossary/search?id=bulk-richardson-number1</a> ).
<b>br1mod (S19)</b>	The BRN was calculated by the same method as <b>br1</b> , except values greater than 5.0 were set to 5.0 in order to improve the linear relationship to peak wind speed.
<b>diff.sfc.1k (H1)</b>	Difference between 500-1000 ft and surface-500 ft layer-average wind speeds.

Table 2. Wind speed parameters calculated from XMR soundings. Heights in MSL.	
<i>Parameter name</i>	<i>Description</i>
<b>max.sfc.5h</b>	Maximum wind speed from the surface to 500 ft. (W1)
<b>max.sfc.1k</b>	Maximum wind speed from the surface to 1000 ft. (W2)
<b>max.sfc.2k</b>	Maximum wind speed from the surface to 2000 ft. (W3)
<b>max.sfc.3k</b>	Maximum wind speed from the surface to 3000 ft. (W4)
<b>max.1k.2k</b>	Maximum wind speed between 1000 ft and 2000 ft. (W5)
<b>max.2k.3k</b>	Maximum wind speed between 2000 ft and 3000 ft. (W6)
<b>ave.sfc.5h</b>	Average wind speed from the surface to 500 ft. (W7)
<b>ave.5h.1k</b>	Average wind speed from 500 ft to 1000 ft. (W8)
<b>ave.sfc.1k</b>	Average wind speed from the surface to 1000 ft. (W9)
<b>ave.1.2k</b>	Average wind speed from 1000 ft to 2000 ft. (W10)
<b>ave.2.3k</b>	Average wind speed from 2000 ft to 3000 ft. (W11)
<b>X16.ft to X3000.ft</b>	Wind speeds at 16 ft through 3000 ft. (W12 - W42)
<b>spdmixL1</b>	Wind speed at the height defined by <b>mixhgtL1</b> . (W43)
<b>spdmixL2</b>	Wind speed at the height defined by <b>mixhgtL2</b> . (W44)
<b>spdmixT</b>	Wind speed at the height defined by <b>mixhgtT</b> . (W45)
<b>maxspdL1</b>	Maximum wind speed from the surface to the height defined by <b>mixhgtL1</b> . (W46)
<b>maxspdL2</b>	Maximum wind speed from the surface to the height defined by <b>mixhgtL2</b> . (W47)
<b>maxspdT</b>	Maximum wind speed from the surface to the height defined by <b>mixhgtT</b> . (W48)

The data set was stratified using the synoptic weather pattern, low-level wind direction, precipitation, Richardson Number and Gradient Richardson Number, for a total of 60 stratification methods. The total number of observation days in each stratification method varied due to missing or undefined data. For example, if the wind shear was zero, the Richardson and Gradient Richardson numbers could not be calculated.

The AMU wrote scripts in the S-PLUS programming language to calculate the least-squares single linear regression equations for the PWSD, AWS D and the timing of the PWSD. Based on the lowest MAE of the equations, the best predictors were selected to create multiple linear regression equations. Single and multiple linear regression equations were also created using robust functions in S-PLUS. Unlike least-squares functions, robust functions reduce the influence of data outliers, while still providing a good fit to most of the data points (Insightful, 2007).

### 3.3 Prediction Equations for PWSD and AWSD

Figure 8 shows the MAE values for predicting the PWSD and AWSD, using least-squares single linear regression equations. The predictors shown on the x-axis include the stability parameters (S1 - S19), wind speed parameters (W1 - W48) and the wind shear parameter (H1). The mean MAE values (in blue) were calculated for each stratification method, and then all 60 stratification methods were averaged together. The minimum MAE values (in red) were the lowest values from all stratification methods. The wind speed parameters performed the best, since they had the lowest MAE values.

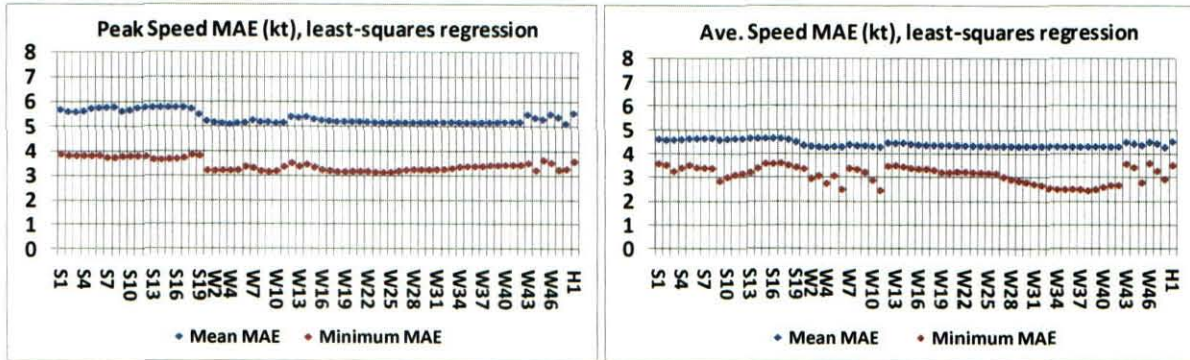


Figure 8. MAE values for least-squares single linear regression equations for PWSD (left) and AWSD (right). The MAE is shown for the stability parameters (S1-S19), wind speed parameters (W1-W48) and wind shear parameter (H1). Mean MAE (blue) is the average of all stratification methods, while Minimum MAE (red) is the lowest of all stratification categories.

Figure 9 shows the MAE values for predicting PWSD and AWSD, using robust single linear regression equations. The robust method is the “lmRobMM” function in the S-PLUS language. The lmRobMM function creates an equation with the following features:

- The data fit to the equation are minimally influenced by outliers and
- The equation minimizes the maximum possible bias of the coefficient estimate (i.e. the slope of the line).

The wind speed parameters performed the best, with the lowest MAE values. The minimum MAE values (in red) were similar for PWSD and AWSD, but the mean MAE values (in blue) for AWSD were lower.

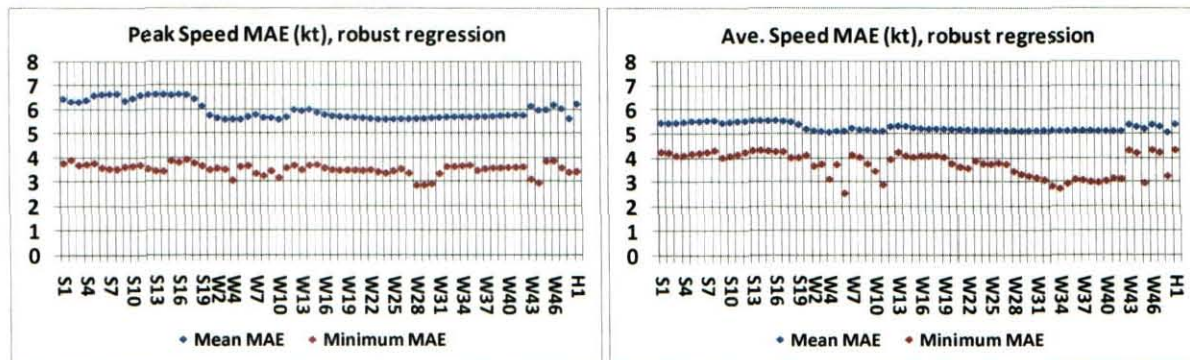


Figure 9. MAE values for robust single linear regression equations for PWSD (left) and AWSD (right). The MAE is shown for the stability parameters (S1-S19), wind speed parameters (W1-W48) and wind shear parameter (H1). Mean MAE (blue) is the average of all stratification categories, while Minimum MAE (red) is the lowest of all stratification categories.

The MAE value for each stratification method was calculated by averaging the MAE values from all 68 stability, wind speed and wind shear parameters. The MAE values were weighted by the size of the categories in the stratification methods.

Figure 10 shows the least-squares method (in blue) performed better than the robust method (in red), with MAE values between 0.5 and 1.0 kt less than the robust method.

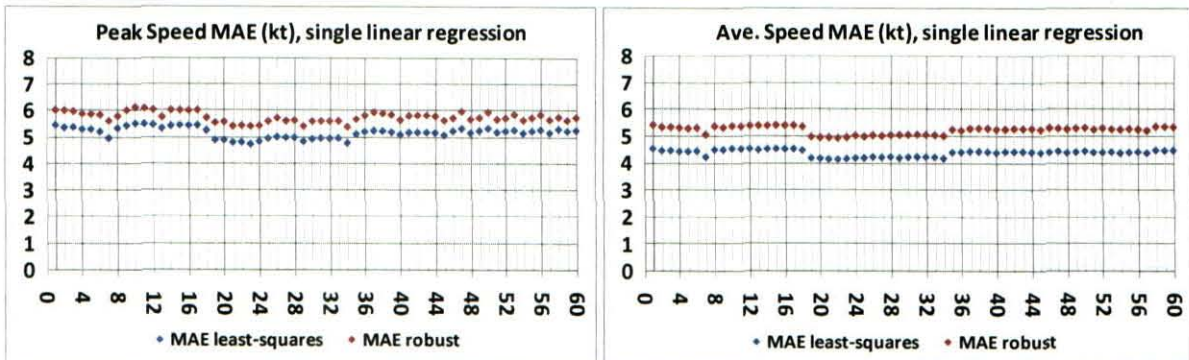


Figure 10. Mean MAE values for least-squares (blue) and robust (red) single linear regression equations for PWSD (left) and AWS D (right). The MAE is shown for the 60 stratifications (x-axis).

Three different multiple linear regression methods were evaluated: least-squares, robust and least-trimmed squares. The least-squares method uses the “step” function in S-PLUS. The step function performs a stepwise multiple linear regression to determine which predictors to use in the regression equation. Due to limitations of the S-PLUS software, only 26 predictors (out of 68) were evaluated by the step function: S1-S6, S9-S12, S19, W2-W6, W8-W11, W22, W27, W32, W37, W48 and H1. The 26 predictors were chosen based on their performance in the single linear regression equations.

The robust method combined the step function with the “lmRob” function in S-PLUS. The lmRob function is similar to the lmRobMM function, and is available from the Robust library in S-PLUS. The S-PLUS 6 Robust Library User’s Guide explains the use of the lmRob function (Insightful, 2002). The lmRob function only used 10 predictors (S1-S4, S19, W4, W6, W11, W37 and W48), due to the limitations of the S-PLUS software. The 10 predictors were chosen based on their performance in the single linear regression equations.

The least-trimmed squares method is similar to the least squares regression, and it is implemented by the “ltsreg” function in S-PLUS. The ltsreg function first removes observations corresponding to large errors to the linear fit. It then calculates a least squares regression equation using the remaining observations. The ltsreg function used the same 10 predictors as the robust method. Unlike the least-squares and robust methods, the ltsreg function does not use stepwise regression to determine which predictors to use in the multiple regression equations. Instead, 10 predictors were used in each least-trimmed squares regression equation.

Figure 11 shows the MAE values of PWSD and AWS D for the three multiple linear regression methods. The values from the least-squares (in blue) and least-trimmed squares (in green) methods were almost identical and overlap in the chart, while the robust (in red) method had MAE values higher than the other two methods.

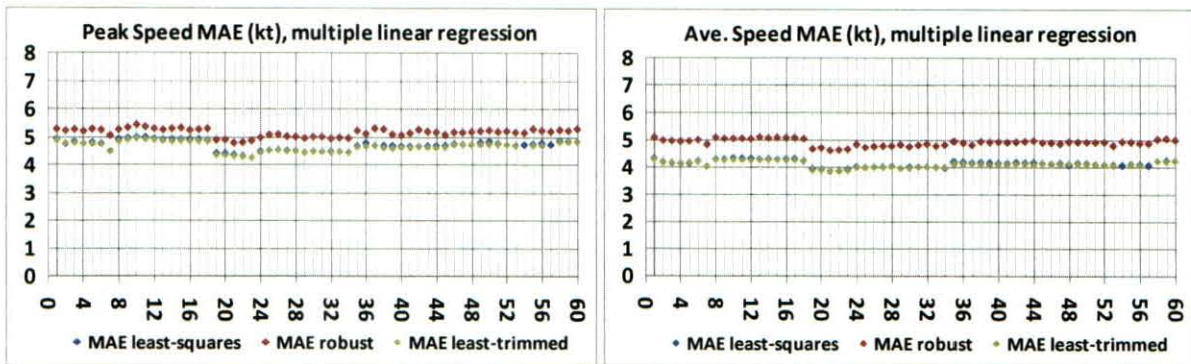


Figure 11. Mean MAE values for least-squares (blue), robust (red) and least-trimmed squares (green) multiple linear regression equations for PWSD (left) and AWSD (right). The MAE is shown for the 60 stratifications (x-axis).

### 3.4 Timing of PWSD

The prediction equations for the timing of the PWSD predict the number of hours elapsed since the beginning of the forecast period at 1300 UTC on the current day. The number of hours that have elapsed can then be converted to clock time, in UTC. For example, if an equation predicts 17 hours have elapsed, then the PWSD is expected to occur at 0600 UTC (or 0100 EST).

Figure 12 shows the MAE (in hours) for predicting the timing of the PWSD, using least-squares (left) and robust (right) single linear regression equations. The mean MAE values (in blue) were the average from all stratification methods, and the minimum MAE values (in red) were the lowest values from all stratifications. There was little difference in MAE among the 68 predictors. The mean coefficient of determination ( $R^2$ ) values were below 0.1, indicating the regression equations provided little skill in predicting the timing of the PWSD (figures not shown).

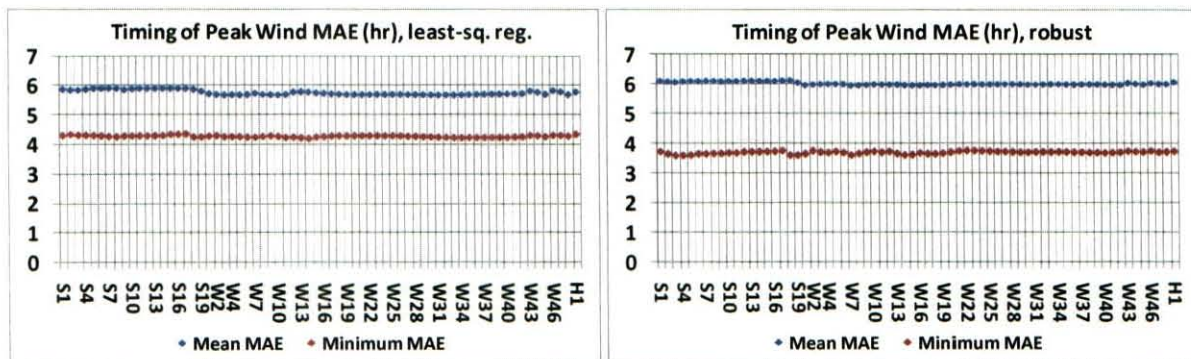


Figure 12. MAE values for least-squares (left) and robust (right) single linear regression equations for timing of the PWSD. The values are shown for the stability parameters (S1-S19), wind speed parameters (W1-W48) and wind shear parameter (H1). Mean MAE (blue) is the average of all stratification methods. Minimum MAE (red) is the lowest of all stratification categories.

Figure 13 shows the MAE values for the 60 stratification methods, for single (left) and multiple (right) linear regressions. All of the linear regressions performed about the same, with MAE values mostly between 5.5 and 6.0 hours.

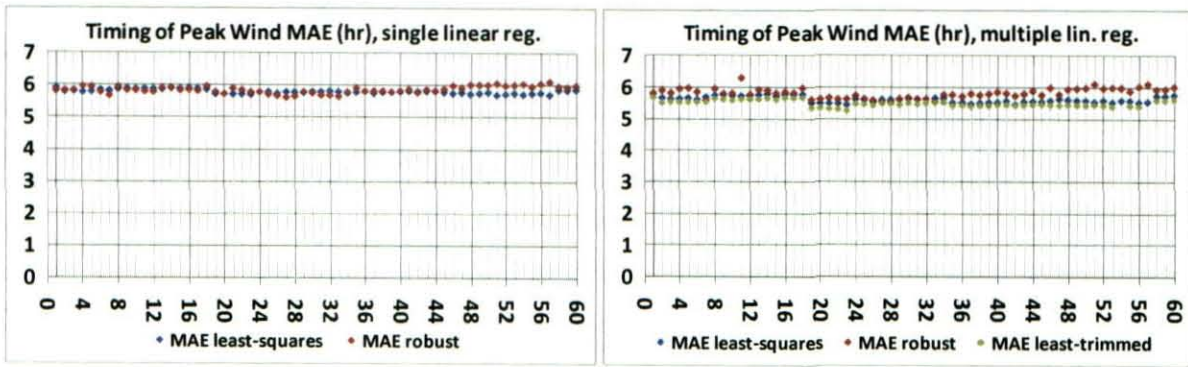


Figure 13. Mean MAE values for single (left) and multiple (right) linear regression equations for timing of the peak wind. The least squares and robust regressions are in blue and red, while the least-trimmed regressions are in green. The values are shown for the 60 stratifications (x-axis).

## 4 Independent Verification of Prediction Methods

The Phase II developmental data set used observations from October 1996 to February 2007, while the Phase I data set used observations from October 2002 to February 2007. An independent verification data set was used to compare the Phase I and II prediction methods to climatology, model forecast winds and wind advisories issued by the 45 WS. The verification data set used observations from March 2007 to April 2009. The prediction methods showing the greatest skill in the verification data set were chosen for the Phase II version of the tool.

Several Phase II prediction methods for the three forecast parameters (PWSD, AWSD and timing of the PWSD) were selected for the independent verification based on the lowest MAE values in the developmental data set. The difficulty or subjectivity in how the predictors were calculated also affected the selection, to make it easier to automate the tool. For example, the prediction methods using the synoptic weather pattern performed well, however the classification of the weather pattern is somewhat subjective. Two trained, experienced forecasters could classify the weather pattern on a given day differently. In addition, stratification methods with more than 10 categories were not selected in order for each category to have a sufficiently large sample size. The stratification methods for precipitation and low-level wind direction performed well in the Phase II methods, so they were selected for the verification. The stratification “none”, which included all days in the Phase II data set, was used as a control in the verification.

Table 3 shows the 30 Phase II prediction methods selected for the verification of PWSD, AWSD and timing of the PWSD, based on five linear regression types and six stratification methods. For predicting the timing of the PWSD, the multiple linear regression equations did not perform significantly better than the single linear regression equations. Therefore, the multiple linear regressions were not independently verified for the timing of the PWSD. These regressions are indicated in red in the left column of Table 3. Table 4 describes the stratification categories for each stratification method listed in Table 3. Table 5 lists the predictor for each single linear regression equation for PWSD, and Table 6 lists the predictors for the multiple linear regression equations.

Table 3. Phase II methods verified for PWSD, AWSD and timing of the PWSD. Methods in red were not verified for the timing of the PWSD.

<i>Method Name</i>	<i>Regression Type</i>	<i>Stratification Method</i>
<b>precip1.best</b>	Least-squares single linear	By precipitation and wind direction: NE, SE, SW and NW (SM1)
<b>precip2.best</b>	Least-squares single linear	By precipitation and wind direction: N, E, S and W (SM2)
<b>precip3.best</b>	Least-squares single linear	By precipitation and wind direction: NE, SE, SW, NW and wind speed $\leq 6.0$ kt (SM3)
<b>precip4.best</b>	Least-squares single linear	By precipitation and wind direction: N, E, S, W and wind speed $\leq 6.0$ kt (SM4)
<b>none.best</b>	Least-squares single linear	No stratification (SM5)
<b>precipcon.best</b>	Least-squares single linear	Mean of the first four stratifications (SM6)
<b>precip1.bestrob</b>	Robust single linear	SM1
<b>precip2.bestrob</b>	Robust single linear	SM2
<b>precip3.bestrob</b>	Robust single linear	SM3
<b>precip4.bestrob</b>	Robust single linear	SM4
<b>none.bestrob</b>	Robust single linear	SM5
<b>precipcon.bestrob</b>	Robust single linear	SM6
<b>precip1.step</b>	Stepwise least-squares multiple linear	SM1
<b>precip2.step</b>	Stepwise least-squares multiple linear	SM2
<b>precip3.step</b>	Stepwise least-squares multiple linear	SM3
<b>precip4.step</b>	Stepwise least-squares multiple linear	SM4
<b>none.step</b>	Stepwise least-squares multiple linear	SM5
<b>precipcon.step</b>	Stepwise least-squares multiple linear	SM6
<b>precip1.steprob</b>	Stepwise robust multiple linear	SM1
<b>precip2.steprob</b>	Stepwise robust multiple linear	SM2
<b>precip3.steprob</b>	Stepwise robust multiple linear	SM3
<b>precip4.steprob</b>	Stepwise robust multiple linear	SM4
<b>none.steprob</b>	Stepwise robust multiple linear	SM5
<b>precipcon.steprob</b>	Stepwise robust multiple linear	SM6
<b>precip1.ltsreg</b>	Least-trimmed multiple linear	SM1
<b>precip2.ltsreg</b>	Least-trimmed multiple linear	SM2
<b>precip3.ltsreg</b>	Least-trimmed multiple linear	SM3
<b>precip4.ltsreg</b>	Least-trimmed multiple linear	SM4
<b>none.ltsreg</b>	Least-trimmed multiple linear	SM5
<b>precipcon.ltsreg</b>	Least-trimmed multiple linear	SM6

Table 4. Stratification categories used in Phase II methods. Wind direction was based on the vector average wind in the lowest 300 ft of XMR sounding. The stratification methods are described in Table 3.

<i>Category / Stratification</i>	<i>Category Description</i>	<i>Category / Stratification</i>	<i>Category Description</i>
C0 / SM5	all days in data set	C18 / SM3	precipitation, SE wind direction, wind speed > 6 kt
C1 / SM1	precipitation, NE wind direction	C19 / SM3	precipitation, SW wind direction, wind speed > 6 kt
C2 / SM1	precipitation, SE wind direction	C20 / SM3	precipitation, NW wind direction, wind speed > 6 kt
C3 / SM1	precipitation, SW wind direction	C21 / SM3&SM4	precipitation, wind speed ≤ 6 kt
C4 / SM1	precipitation, NW wind direction	C22 / SM3	no precipitation, NE wind direction, wind speed > 6 kt
C5 / SM1	no precipitation, NE wind direction	C23 / SM3	no precipitation, SE wind direction, wind speed > 6 kt
C6 / SM1	no precipitation, SE wind direction	C24 / SM3	no precipitation, SW wind direction, wind speed > 6 kt
C7 / SM1	no precipitation, SW wind direction	C25 / SM3	no precipitation, NW wind direction, wind speed > 6 kt
C8 / SM1	no precipitation, NW wind direction	C26 / SM3&SM4	no precipitation, wind speed ≤ 6 kt
C9 / SM2	precipitation, N wind direction	C27 / SM4	precipitation, N wind direction, wind speed > 6 kt
C10 / SM2	precipitation, E wind direction	C28 / SM4	precipitation, E wind direction, wind speed > 6 kt
C11 / SM2	precipitation, S wind direction	C29 / SM4	precipitation, S wind direction, wind speed > 6 kt
C12 / SM2	precipitation, W wind direction	C30 / SM4	precipitation, W wind direction, wind speed > 6 kt
C13 / SM2	no precipitation, N wind direction	C31 / SM4	no precipitation, N wind direction, wind speed > 6 kt
C14 / SM2	no precipitation, E wind direction	C32 / SM4	no precipitation, E wind direction, wind speed > 6 kt
C15 / SM2	no precipitation, S wind direction	C33 / SM4	no precipitation, S wind direction, wind speed > 6 kt
C16 / SM2	no precipitation, W wind direction	C34 / SM4	no precipitation, W wind direction, wind speed > 6 kt
C17 / SM3	precipitation, NE wind direction, wind speed > 6 kt		

Table 5. Stratification category and predictors for each PWSD equation using single linear regression. The stratification categories are described in Table 4.

<i>Method Name</i>	<i>Stratification Category / Predictor</i>	<i>Method Name</i>	<i>Stratification Category / Predictor</i>
precip1.best	C1 / W42	precip1.bestrob	C1 / W42
precip1.best	C2 / W39	precip1.bestrob	C2 / W38
precip1.best	C3 / W18	precip1.bestrob	C3 / S19
precip1.best	C4 / W4	precip1.bestrob	C4 / W3
precip1.best	C5 / W25	precip1.bestrob	C5 / W25
precip1.best	C6 / W24	precip1.bestrob	C6 / W4
precip1.best	C7 / W39	precip1.bestrob	C7 / W35
precip1.best	C8 / W9	precip1.bestrob	C8 / W3
precip2.best	C9 / W12	precip2.bestrob	C9 / W12
precip2.best	C10 / W42	precip2.bestrob	C10 / W42
precip2.best	C11 / W48	precip2.bestrob	C11 / W18
precip2.best	C12 / W37	precip2.bestrob	C12 / W23
precip2.best	C13 / W23	precip2.bestrob	C13 / W3
precip2.best	C14 / W25	precip2.bestrob	C14 / W24
precip2.best	C15 / W4	precip2.bestrob	C15 / W10
precip2.best	C16 / W48	precip2.bestrob	C16 / W10
precip3.best	C17 / W7	precip3.bestrob	C17 / W13
precip3.best	C18 / W5	precip3.bestrob	C18 / W2
precip3.best	C19 / S18	precip3.bestrob	C19 / S19
precip3.best	C20 / W30	precip3.bestrob	C20 / W3
precip3.best	C21 / W37	precip3.bestrob	C21 / W38
precip3.best	C22 / W25	precip3.bestrob	C22 / W25
precip3.best	C23 / W24	precip3.bestrob	C23 / W4
precip3.best	C24 / W38	precip3.bestrob	C24 / W38
precip3.best	C25 / W9	precip3.bestrob	C25 / W9
precip3.best	C26 / W3	precip3.bestrob	C26 / W28
precip4.best	C27 / W48	precip4.bestrob	C27 / W3
precip4.best	C28 / W42	precip4.bestrob	C28 / W13
precip4.best	C29 / W1	precip4.bestrob	C29 / W18
precip4.best	C30 / W42	precip4.bestrob	C30 / W42
precip4.best	C21 / W37	precip4.bestrob	C21 / W38
precip4.best	C32 / W8	precip4.bestrob	C32 / W8
precip4.best	C33 / W25	precip4.bestrob	C33 / W9
precip4.best	C34 / W24	precip4.bestrob	C34 / W24
precip4.best	C35 / W48	precip4.bestrob	C35 / W48
precip4.best	C26 / W3	precip4.bestrob	C26 / W28
none.best	C0 / W4	none.bestrob	C0 / W3

Table 6. Stratification category and predictors for each PWS equation using multiple linear regression. The stratification categories are described in Table 4.

<i>Method Name</i>	<i>Stratification Category / Predictor(s)</i>	<i>Method Name</i>	<i>Stratification Category / Predictor(s)</i>
precip1.step	C1 / S2, W4, W5, W11	precip1.steprob	C1 / S1, W4, W11
precip1.step	C2 / W6	precip1.steprob	C2 / S1, W37
precip1.step	C3 / S19, W9	precip1.steprob	C3 / S3, S4, S19, W6, W11
precip1.step	C4 / W37	precip1.steprob	C4 / S19, W4
precip1.step	C5 / W10	precip1.steprob	C5 / S19, W11
precip1.step	C6 / S9, W8	precip1.steprob	C6 / W4, W6, W11
precip1.step	C7 / S11, W11	precip1.steprob	C7 / S2, S3, W11
precip1.step	C8 / S10, W9, W48	precip1.steprob	C8 / S3, W6, W48
precip2.step	C9 / S5, W3, W48	precip2.steprob	C9 / S1, S19, W4
precip2.step	C10 / S2, W11	precip2.steprob	C10 / S1, W11
precip2.step	C11 / S19, W9, W22, W48	precip2.steprob	C11 / S19, W48
precip2.step	C12 / W37	precip2.steprob	C12 / S2, S3, S4, W6
precip2.step	C13 / S4, S19, W22	precip2.steprob	C13 / S1, S2, S3, W48
precip2.step	C14 / H1, S12, S19, W2, W5, W22, W32, W37	precip2.steprob	C14 / S4, S19, W4, W6, W11, W37
precip2.step	C15 / S2, W4, W9	precip2.steprob	C15 / S2, S3, S19, W4, W6, W11
precip2.step	C16 / W9, W48	precip2.steprob	C16 / S4, W6, W37, W48
precip3.step	C17 / S1, W2, W3, W4	precip3.steprob	C17 / S4, S19, W4
precip3.step	C18 / W5	precip3.steprob	C18 / S1, W4, W6, W37
precip3.step	C19 / W48	precip3.steprob	C19 / S3, S4, S19, W6
precip3.step	C20 / S4, S5, W37	precip3.steprob	C20 / S4, S19, W4, W6, W11
precip3.step	C21 / S19, W10, W37	precip3.steprob	C21 / S2, W11, W37
precip3.step	C22 / W5	precip3.steprob	C22 / S1, S2, S3, W11, W48
precip3.step	C23 / W8	precip3.steprob	C23 / W4, W6, W11
precip3.step	C24 / S12, W11	precip3.steprob	C24 / S2, S3, W11
precip3.step	C25 / S9, W6, W9, W48	precip3.steprob	C25 / S1, S3, W6, W48
precip3.step	C26 / S5, S12, W11	precip3.steprob	C26 / S1, S3, S4, W4, W6, W37
precip4.step	C27 / S5, S19, W48	precip4.steprob	C27 / S4, S19, W48
precip4.step	C28 / S4, S10, W11	precip4.steprob	C28 / S4, W6, W11, W48
precip4.step	C29 / W9, W22, W48	precip4.steprob	C29 / S2, S3, W48
precip4.step	C30 / S9, W32, W37	precip4.steprob	C30 / S2, S3, S4, W4
precip4.step	C31 / S19, W10, W37	precip4.steprob	C31 / S2, W11, W37
precip4.step	C32 / S9, W3, W6, W8	precip4.steprob	C32 / S3, W37, W48
precip4.step	C33 / W2, W3, W9, W32, W37	precip4.steprob	C33 / S1, S2, S3, S19, W4, W6, W11, W37
precip4.step	C34 / S2, S12, W2	precip4.steprob	C34 / S2, S3, S19, W4
precip4.step	C35 / S11, W48	precip4.steprob	C35 / S1, W48
precip4.step	C36 / S5, S12, W11	precip4.steprob	C36 / S1, S3, S4, W4, W6, W37
none.step	C0 / S10, S12, W4, W6, W9, W37	none.steprob	C0 / S1, S2, S3, W4, W6, W11

## 4.1 Peak and Average Wind Speed

The Phase I and II prediction methods for PWSD and AWSD were compared to climatology and the 0000 and 1200 UTC runs of the 12-km North American Mesoscale (MesoNAM) model. Comparisons were done for precipitation and non-precipitation days in the verification data set. Then, the Phase I and II prediction methods for PWSD were compared to wind advisories issued by the 45 WS.

### 4.1.1 Comparing Phase I and II Methods to Climatology

The Phase I and II prediction methods for PWSD and AWSD were first compared to four climatology methods. The prediction methods for PWSD were compared to the climatological PWSD (surface to 300 ft), while the prediction methods for AWSD were compared to the climatological AWSD (surface to 300 ft). The climatological peak/average wind speeds were also based on the mean peak/average wind speeds at 54 ft, 90 ft and 204 ft calculated in a previous AMU task (Lambert 2002).

Figure 14 shows the mean error for PWSD (left) and AWSD (right) for days without precipitation. The Phase II climatological winds (point 4, in dark blue) had a positive bias around 2 kt, while the climatological winds at 54 ft, 90 ft and 204 ft (points 1-3, in dark blue) had large negative biases. The Phase I and II methods generally had a slight negative bias. Figure 15 shows the mean error for PWSD (left) and AWSD (right) for days with precipitation. There was a negative bias in the Phase I and II methods, indicating the methods under-predict the PWSD and AWSD on precipitation days.

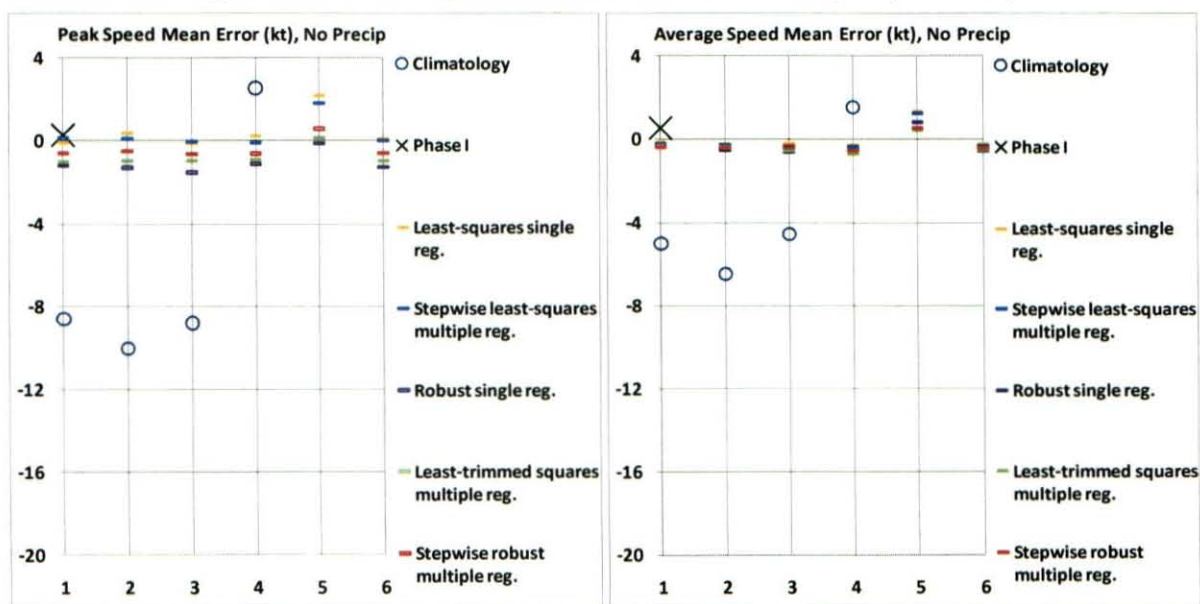


Figure 14. Mean Error for PWSD (left) and AWSD (right) on non-precipitation days For the Phase II methods, points 1-6 (on x-axis) correspond to stratification methods SM1-SM6, respectively. The legend describes the colors corresponding to the Phase II linear regression types. Refer to Table 3 for a description of the stratification methods and linear regression types. The climatology methods are plotted on points 1-4. The Phase I method is plotted on point 1.

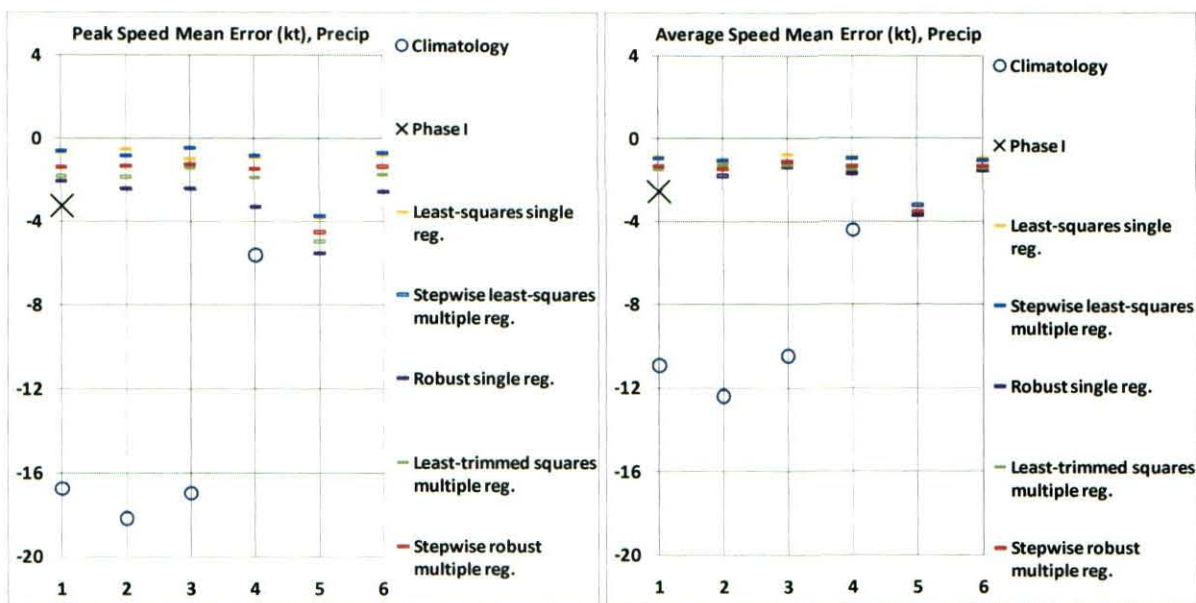


Figure 15. Mean Error for PWS (left) and AWS (right) on precipitation days, for the climatology and Phase I and II methods. Refer to Figure 14 for a description of the x-axis.

Figure 16 shows the MAE for PWS (left) and AWS (right) for days without precipitation. The Phase I and II methods had very similar MAE values. Figure 17 shows the MAE for PWS (left) and AWS (right) for days with precipitation. Similar to Figure 16, the MAE values from the Phase I and II methods were similar, with the Phase II “SMS” stratification (point 5) having the highest MAE values. Comparing Figure 16 and Figure 17, the MAE values were higher on precipitation days.

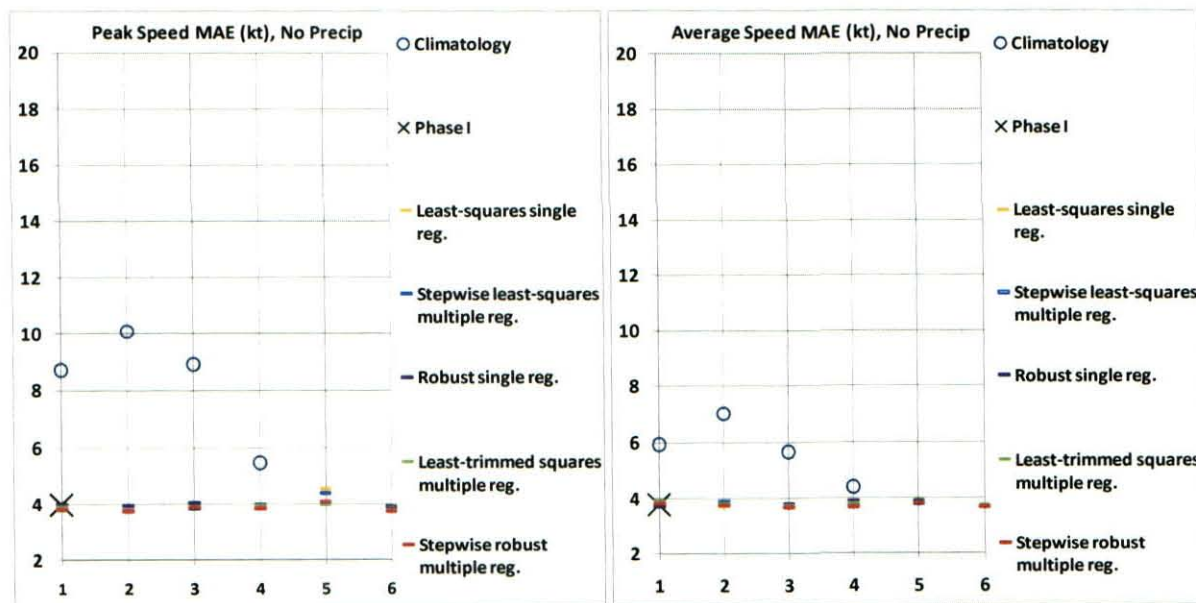


Figure 16. MAE for PWS (left) and AWS (right) on non-precipitation days, for the climatology and Phase I and II methods. Refer to Figure 14 for a description of the x-axis.

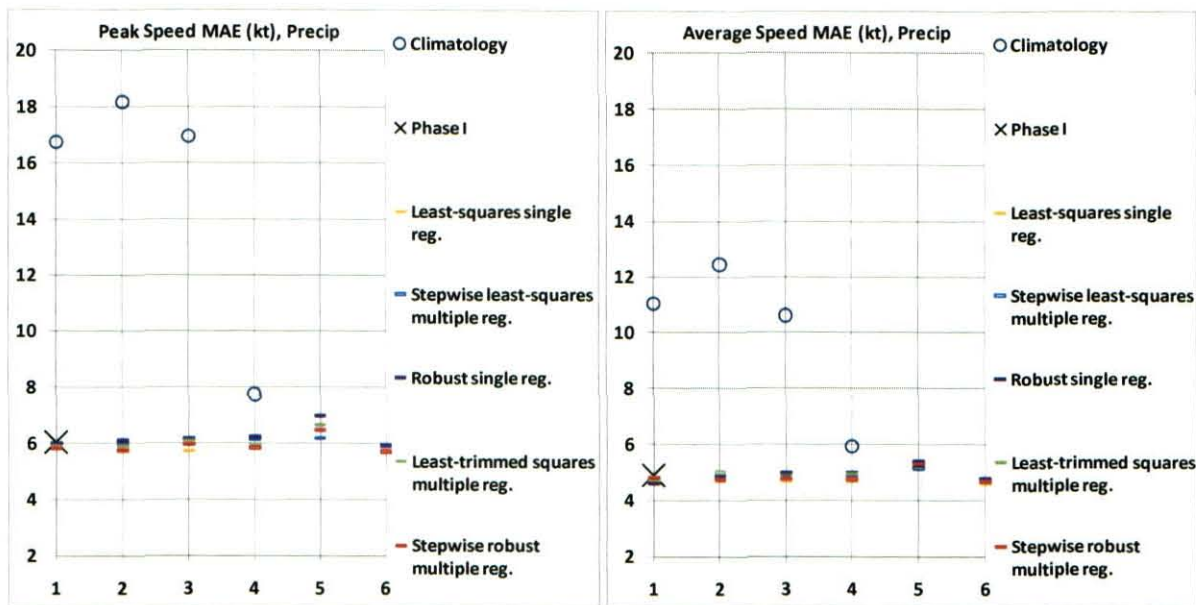


Figure 17. MAE for PWSD (left) and AWSD (right) on precipitation days, for the climatology and Phase I and II methods. Refer to Figure 14 for a description of the x-axis.

The relationship between mean error, MAE and precipitation was investigated further. Most of the days with large absolute errors had precipitation (figures not shown). The large errors could be due to convective wind gusts, since the Wind Tower QC program did not filter out all of the convective wind gusts. Some of the non-precipitation days with large errors in PWSD and AWSD might actually have had rainfall over the forecast area. A day with precipitation was defined as having at least one observation at SLF with precipitation, thunder, or a shower within 5 NM. It is possible some days had precipitation across KSC or CCAFS, but not within 5 NM of the SLF.

Figure 18 shows the mean error when the absolute error for PWSD was within 5 kt (left) and greater than 5 kt (right). The figure shows a bias near zero when the absolute error was  $\leq 5$  kt, but large negative bias when the absolute error was  $> 5$  kt. This indicates the negative bias in PWSD becomes greater as the absolute error increases. There was also a much greater spread between the Phase I and II methods when the absolute error was greater than 5 kt. Figure 19 shows the mean error when the absolute error for AWSD was  $\leq 5$  kt (left) and  $> 5$  kt (right). Similar to Figure 18, the negative bias in AWSD was greater when the absolute error was  $> 5$  kt. However, the spread between the Phase I and II methods was not as large. The negative bias was even greater for PWSD and AWSD when the absolute error was  $> 8$  kt (figure not shown).

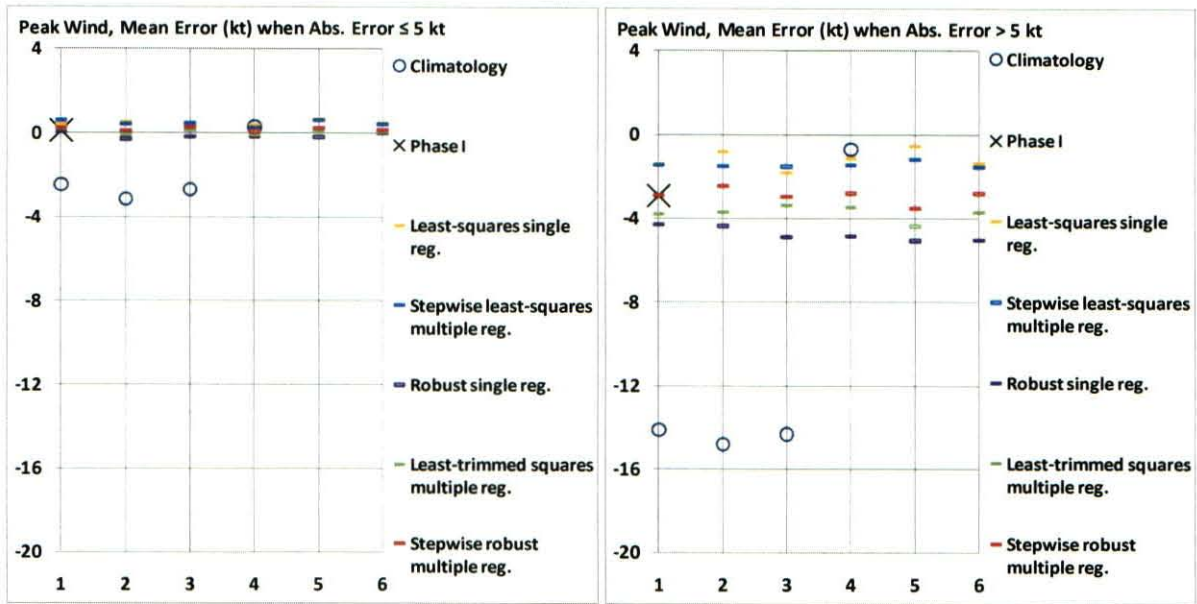


Figure 18. Mean Error for PWSD on days in which the forecast's absolute error is within 5 kt (left) and greater than 5 kt (right). Refer to Figure 14 for a description of the x-axis.

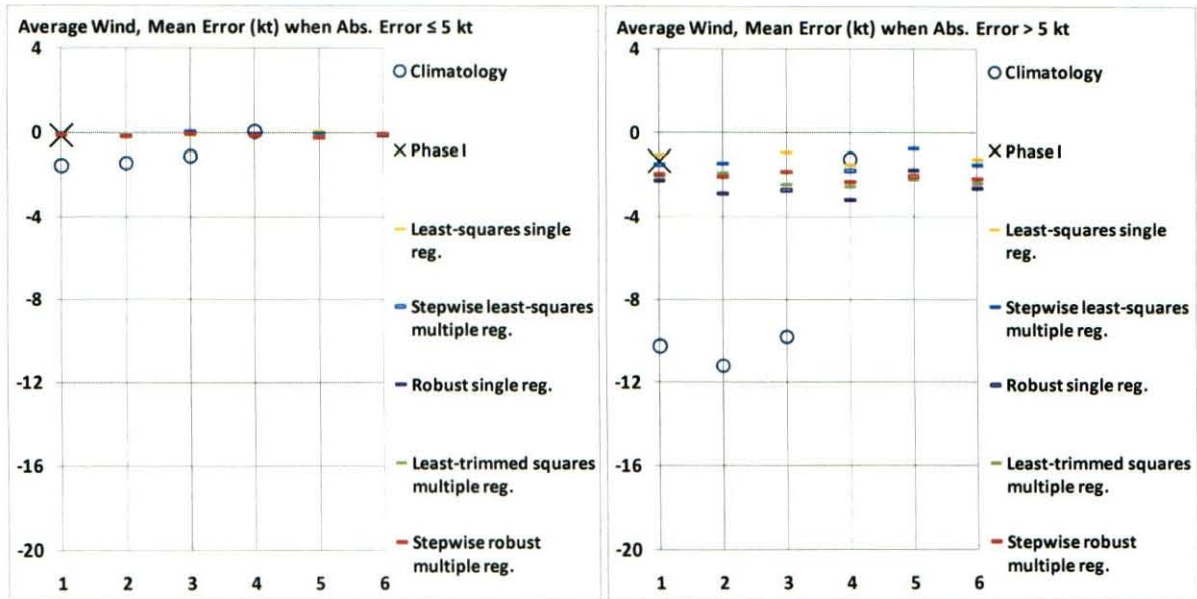


Figure 19. Mean Error for AWSD on days in which the forecast's absolute error is within 5 kt (left) and greater than 5 kt (right). Refer to Figure 14 for a description of the x-axis.

A relationship was found between the absolute error of the Phase I and II equations for PWSD, and the difference between PWSD and the tower-average peak speed. As noted in Section 2.1, the PWSD was the highest peak speed (surface to 300 ft) of all the KSC/CCAFS towers used in the task, during a 24-hour period. The tower-average peak speed is the average of the 24-hour peak speeds (surface to 300 ft) for all of the towers. Figure 20 shows the average difference between the PWSD and the tower-average peak speed, for days in which the absolute error was  $\leq 5$  kt (left) and  $> 5$  kt (right). As the absolute error increased, the difference between the PWSD and the tower-average peak speed increased. The increase continued when the absolute error was  $> 8$  kt (figure not shown). In other words, the difference between the PWSD and the tower-average peak speed was related to the predictability of the PWSD. The cause of

this effect may be due to wind gusts that only affect a portion of the KSC/CCAFS tower network. Measurement errors in the tower network could also contribute to the difference between the PWSD and tower-average peak speed. It is possible the absolute error also increases with the magnitude of the PWSD, but this was not investigated.

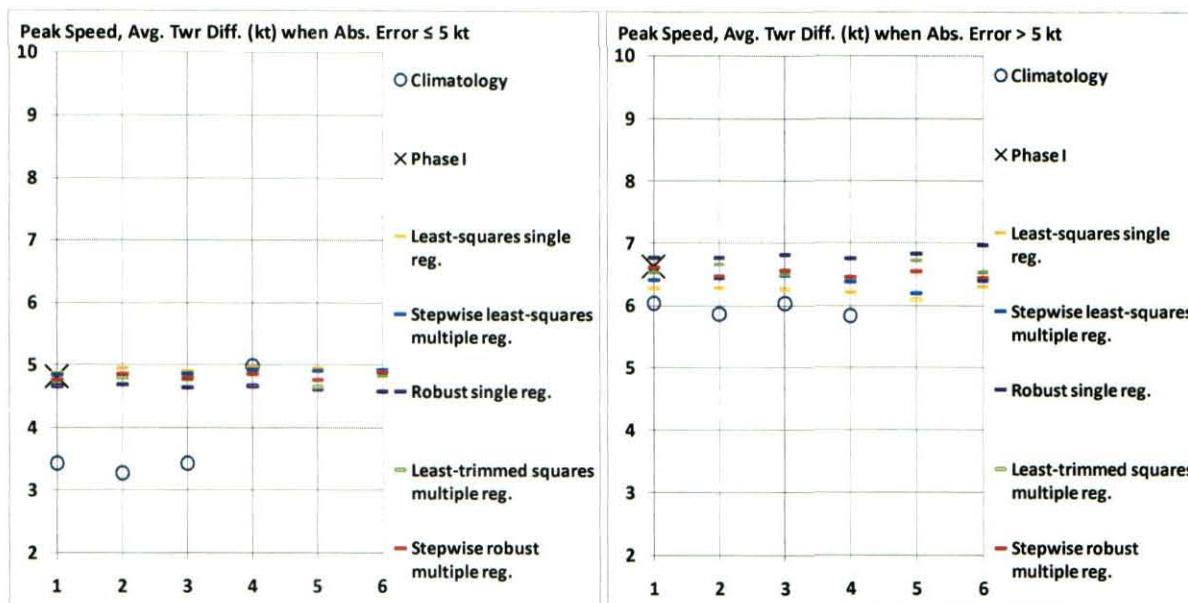


Figure 20. Average difference between the PWSD and the tower-average peak speed, on days in which the forecast's absolute error is within 5 kt (left) and greater than 5 kt (right). Refer to Figure 14 for a description of the x-axis.

#### 4.1.2 Comparing Phase I and II Methods to Model Forecast Winds

The Phase I and II methods for predicting PWSD and AWS D were then compared to model forecast winds. The Phase I and II methods for predicting PWSD and AWS D were then compared to model forecast winds. The model forecast winds were derived from 0000 and 1200 UTC runs of the MesoNAM. The MesoNAM contained hourly forecasts out to 84 hours, although the independent verification only used the Day-1 (1300 UTC to 1300 UTC) forecasts. The comparison used the MesoNAM wind data for the grid point closest to the XMR sounding. Levels 2 to 18 of the MesoNAM were evaluated, along with the strongest winds in the lowest 1000-, 2000- and 3000-ft of the model. The height of each model level varied by forecast hour and model run, due to changes in surface pressure and temperatures aloft. Table 7 shows the average and standard deviation of the heights for the MesoNAM levels 2 - 18, based on the verification data set. Two sets of MesoNAM forecasts were used in the comparison. The first set included the strongest wind at each model level during the 24-hour period. The second set used least-squares single linear regression equations, in which the predictor was the model level's highest 24-hour peak speed and the predictand was the PWSD or AWS D.

Table 7. Average heights and standard deviations of the MesoNAM vertical levels used in the verification data.					
Level	Average Height (MSL)	Standard Deviation of Height	Level	Average Height (MSL)	Standard Deviation of Height
2	207 ft	4 ft	11	1571 ft	23 ft
3	344 ft	5 ft	12	1751 ft	25 ft
4	483 ft	7 ft	13	1940 ft	28 ft
5	626 ft	9 ft	14	2140 ft	31 ft
6	772 ft	12 ft	15	2352 ft	34 ft
7	922 ft	14 ft	16	2583 ft	37 ft
8	1076 ft	16 ft	17	2842 ft	41 ft
9	1234 ft	18 ft	18	3145 ft	45 ft
10	1399 ft	20 ft			

Figure 21 shows the mean error for PWSD (left) and AWSD (right) of the Phase I and II, climatology, and MesoNAM forecasts. Only the 0000 UTC MesoNAM is shown, since there were only minor differences between the 0000 and 1200 UTC runs of the model. The Phase I and II methods generally had a weak negative bias. The strongest 24-hour MesoNAM forecast winds at each level are shown in black, and their bias varied by model level. The MesoNAM linear regression forecasts are shown in light blue, and their bias was zero. Figure 22 shows the MAE for PWSD (left) and AWSD (right). The MesoNAM linear regression forecasts were the most accurate, especially at the lower model levels.

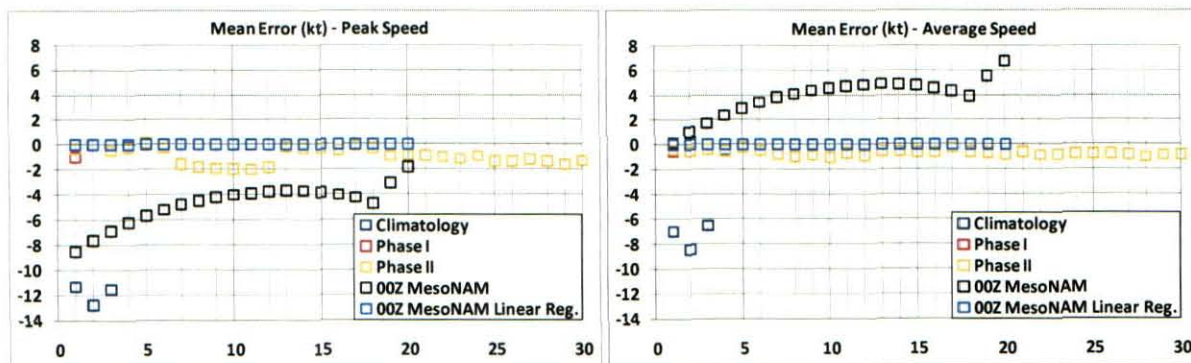


Figure 21. Mean Error for PWSD and AWSD. The strongest 24-hour 0000 UTC MesoNAM forecast winds are plotted on points 1-20, in black. The 0000 UTC MesoNAM linear regression forecasts are plotted on points 1-20, in light blue. The climatology methods are plotted on points 1-4, in dark blue. The Phase I method is plotted on point 1 (in red), and the Phase II methods are plotted on points 1-30 (in yellow). Refer to Table 3 for a description of the Phase II methods

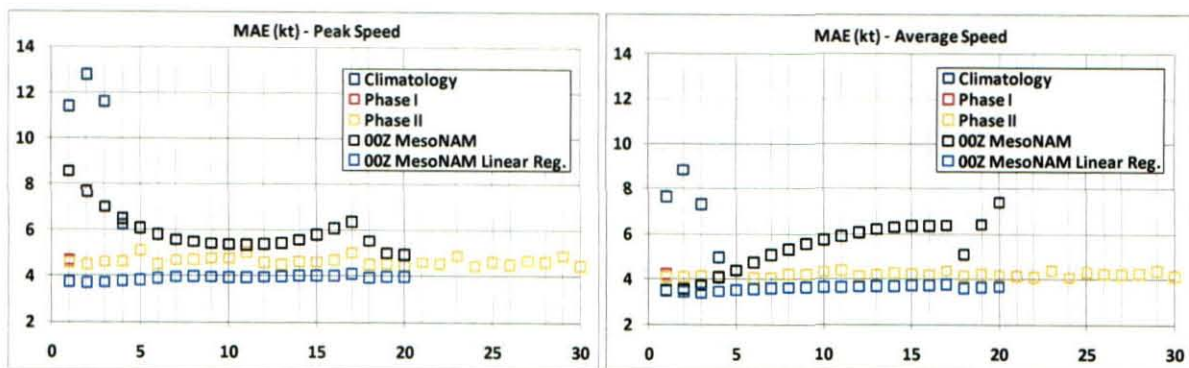


Figure 22. MAE for PWSD and AWS. Refer to Figure 21 for a description of the x-axis.

Figure 23 shows the mean error for PWSD for days with (left) and without precipitation (right). For the MesoNAM data, separate regression equations were not developed for precipitation and non-precipitation days. The MesoNAM regression forecasts (in light blue) had a negative bias around 2 kt on precipitation days and a positive bias around 1 kt on non-precipitation days. Figure 24 shows the mean error for AWS for days with (left) and without precipitation (right). Similar to PWSD, the MesoNAM regression forecasts had a negative bias on precipitation days and a positive bias on non-precipitation days.

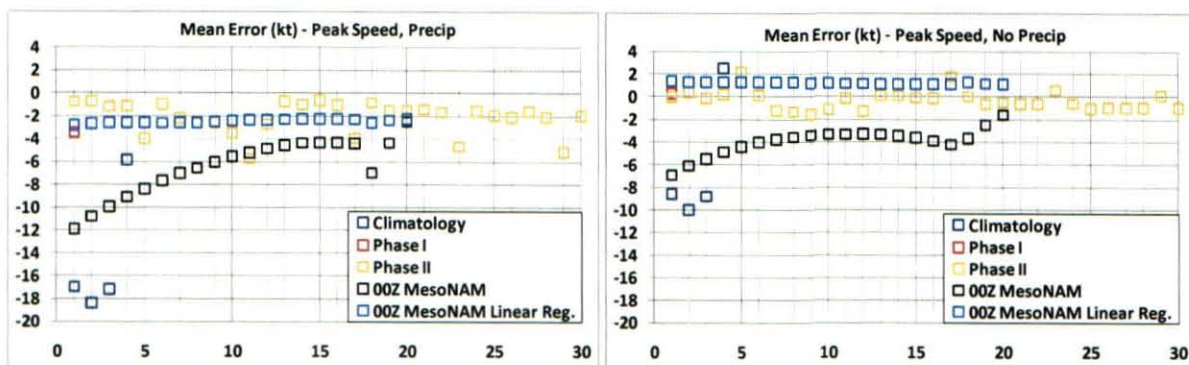


Figure 23. Mean Error for PWSD on precipitation (left) and non-precipitation days (right). Refer to Figure 21 for a description of the x-axis.

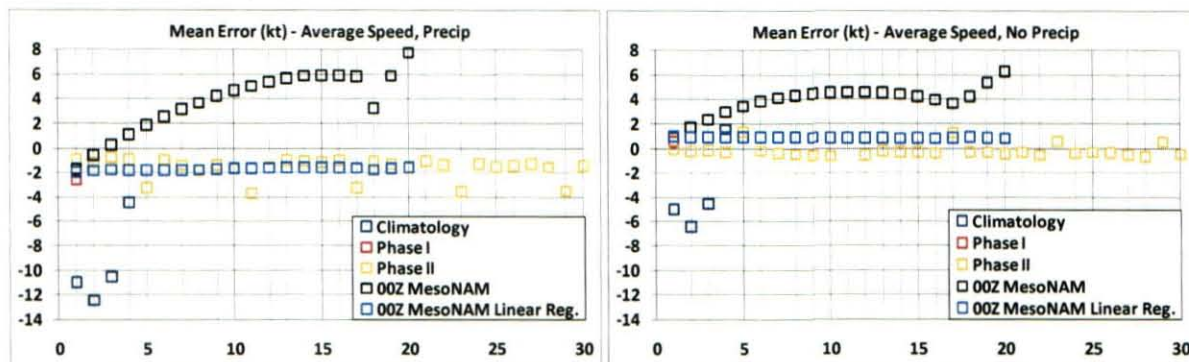


Figure 24. Mean Error for AWS on precipitation (left) and non-precipitation days (right). Refer to Figure 21 for a description of the x-axis.

Figure 25 and Figure 26 show the MAE for PWSD and AWS for days with (left) and without precipitation (right). The MesoNAM regression forecasts performed better than the Phase I and II methods, especially for precipitation days.

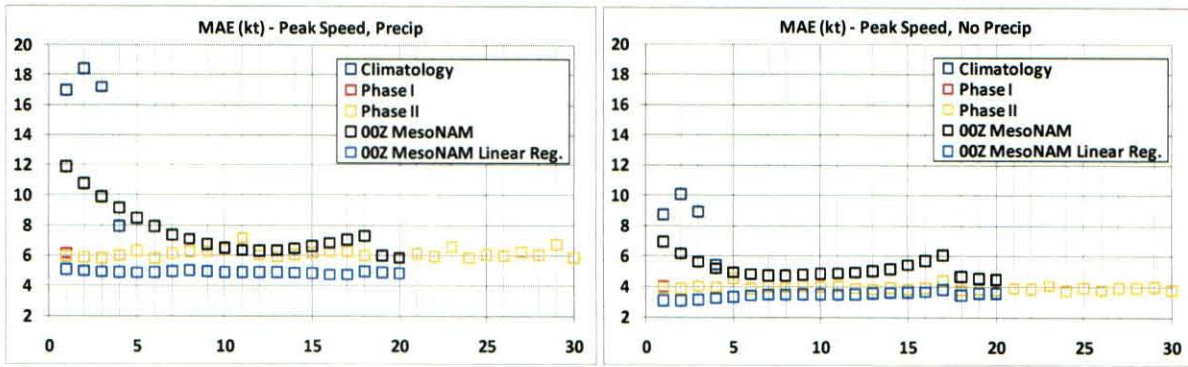


Figure 25. MAE for PWSD on precipitation (left) and non-precipitation days (right). Refer to Figure 21 for a description of the x-axis.

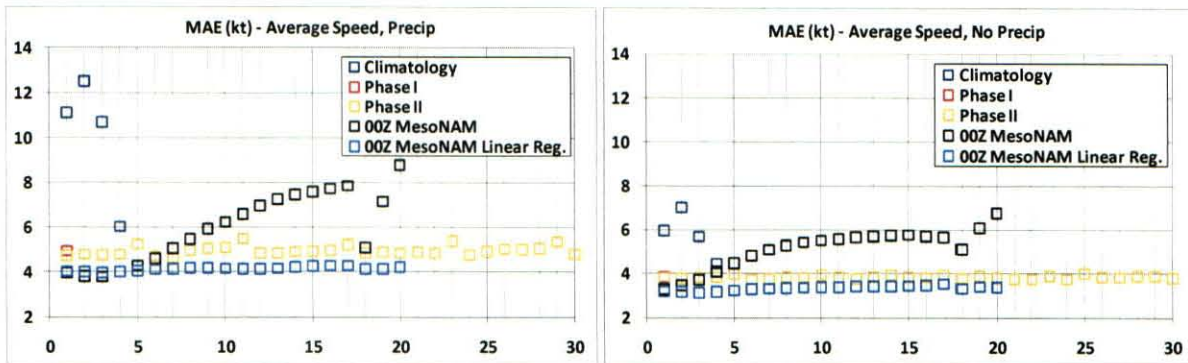


Figure 26. MAE for AWSD on precipitation (left) and non-precipitation days (right). Refer to Figure 21 for a description of the data points.

Figure 27 shows the MAE for PWSD (left) and AWSD (right) from the MesoNAM regression forecasts. On precipitation days, the 1200 UTC model runs (in purple) performed just slightly better than the 0000 UTC model runs (in red). On non-precipitation days, there was virtually no difference between the 0000 UTC (in light blue) and 1200 UTC (in orange) model runs.

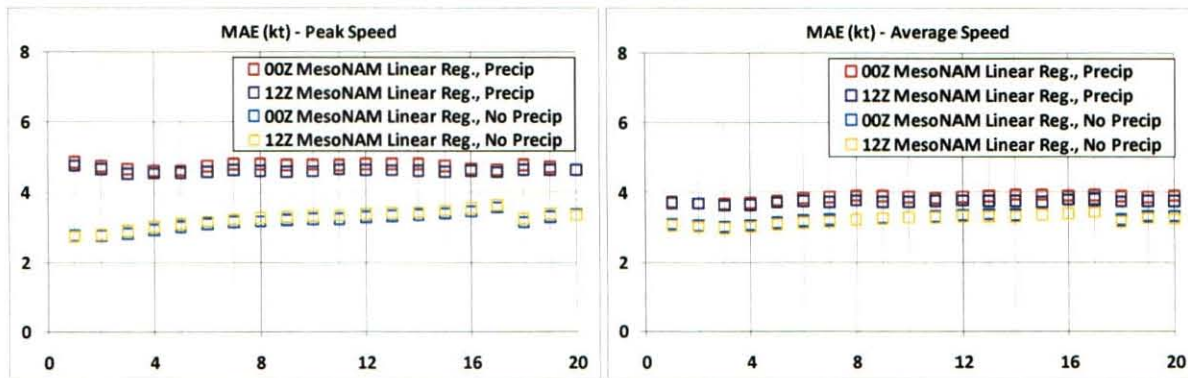


Figure 27. MAE for PWSD (left) and AWSD (right), for 0000 and 1200 UTC MesoNAM regression forecasts. Points 1-17 depict model levels 2-18, and points 18-20 depict the strongest winds in the lowest 1000-, 2000-, and 3000-ft of the model. The legend shows the color corresponding to each method.

The MesoNAM linear regression forecasts were clearly the most accurate in the verification data set. The differences between the 0000 and 1200 UTC model runs were not significant. The Phase I and II

forecasts were similar, although the best Phase II methods were slightly more accurate than the Phase I forecasts. The climatology forecasts performed the worst.

#### 4.1.3 Comparison of Phase I and II Peak Wind Speed Predictions to 45 WS Wind Advisories

The Phase I and II forecasts of PWSD were compared to the 45 WS wind advisories on days in which the 45 WS issued at least one non-convective wind advisory. In addition to KSC and CCAFS, the comparison also included wind advisories for PAFB. There were three types of wind advisories for non-convective peak winds: 25-34 kt, 35-49 kt and 50 kt or greater. The valid time periods for the wind advisories were variable in length, ranging from around one hour to close to two days. Some of the wind advisories extended across multiple 24-hour forecast periods (0800 to 0800 local time). Multiple wind advisories could also be issued during one 24-hour forecast period. For this comparison, if a wind advisory extended across two 24-hour forecast periods, then the comparison analyzed the two days separately. If a 24-hour forecast period included multiple wind advisories, then they were counted as one wind advisory. The comparison used the strongest wind advisory for the forecast period. Wind advisories of the same type and forecast period, but different areas (such as KSC and CCAFS), were merged for the comparison. Also, the comparison did not include wind advisories with a time period of less than four hours, in order to avoid small-scale weather systems.

Table 8 shows the comparison for days in which the strongest wind advisory was for 25-34 kt (left) and 35-49 kt (right). The wind advisories for winds of 50 kt or greater are not shown, since only two warnings meeting the criteria for this comparison (see previous paragraph) were issued during the verification period. A “hit” was defined as an observed PWSD in the correct forecast interval (25-34 kt or 35-49 kt). An “over-forecast” was defined as an observed PWSD weaker than the forecast interval. An “under-forecast” was defined as an observed PWSD stronger than the forecast interval. Table 8 shows the 45 WS out-performed the Phase I and II methods, because the 45 WS had the most hits. On days in which the 45 WS issued a wind advisory for 35-49 kt, they tended to over-forecast more often than under-forecast, while the Phase I and II methods under-forecast more often than they over-forecast.

Table 8. Verification for days in which the highest 45 WS wind warning/advisory was 25-34 kt (left) and 35-49 kt (right). Phase II methods are shown in blue.

<i>Method</i>	25 - 34 kt			35 - 49 kt		
	<i>Hits</i>	<i>Under-forecast</i>	<i>Over-forecast</i>	<i>Hits</i>	<i>Under-forecast</i>	<i>Over-forecast</i>
<b>least-squares single regression</b>	35	13	4	35	29	3
<b>robust single regression</b>	32	19	1	29	36	1
<b>stepwise least-squares regression</b>	36	13	4	33	30	3
<b>stepwise robust regression</b>	34	15	3	34	30	3
<b>least-trimmed squares regression</b>	31	17	4	31	33	3
<b>Phase I</b>	34	16	2	34	31	1
<b>45 WS</b>	45	6	2	41	2	28

## 4.2 Timing of the Peak Wind

As described in the first paragraph of Section 3.4, the timing of the peak wind was defined as the number of hours elapsed since the beginning of the forecast period (1300 UTC). The Phase I and II methods for predicting the timing of the peak wind were compared to six climatology values. The first three climatology values were based on the mean peak winds at 54-, 90- and 204-ft (Lambert 2002). For

each of the three levels, the cool season mean peak wind speed was calculated for each hour of the day. The timing was then defined as the hour in which the highest mean peak wind speed occurred. Table 9 shows the climatological timing of the peak wind. The hours used for this comparison are highlighted in yellow.

Table 9. Climatology methods for predicting timing of the peak wind, based on the mean peak winds in a previous AMU task (Lambert 2002). The “average wind speed” is the average of all the towers used in the previous AMU task, and the “maximum wind speed” is the maximum of all the towers.

<i>Hour in UTC</i>	<i>54 ft / 60ft average wind speed</i>	<i>54 ft / 60 ft maximum wind speed</i>	<i>90 ft average wind speed</i>	<i>90 ft maximum wind speed</i>	<i>204 ft average wind speed</i>	<i>204 ft maximum wind speed</i>
0000	11.03	12.69	11.71	11.73	14.14	14.19
0100	10.94	12.53	11.66	11.68	14.13	14.18
0200	10.88	12.45	11.62	11.63	14.11	14.18
0300	10.76	12.28	11.56	11.57	13.98	14.06
0400	10.62	12.07	11.51	11.53	13.91	14.03
0500	10.47	11.87	11.42	11.43	13.71	13.85
0600	10.39	11.76	11.33	11.33	13.61	13.75
0700	10.24	11.57	11.18	11.18	13.41	13.56
0800	10.14	11.50	11.05	11.06	13.22	13.39
0900	10.16	11.58	10.98	10.99	13.19	13.37
1000	10.14	11.58	10.94	10.96	13.18	13.37
1100	10.10	11.51	10.88	10.89	13.07	13.26
1200	10.36	11.71	10.96	10.98	13.13	13.36
1300	11.21	12.40	11.48	11.48	13.25	13.42
1400	12.31	13.42	12.37	12.38	13.67	13.79
1500	13.18	14.38	13.08	13.11	14.26	14.33
1600	13.75	15.07	13.47	13.51	14.74	14.79
1700	14.09	15.37	13.77	13.81	15.07	15.09
1800	14.24	15.50	13.98	14.04	15.28	15.28
1900	14.10	15.35	13.99	14.06	15.22	15.22
2000	13.76	15.11	13.71	13.79	15.05	15.05
2100	13.06	14.51	13.20	13.26	14.65	14.66
2200	12.03	13.63	12.30	12.35	14.26	14.28
2300	11.27	12.97	11.77	11.80	14.09	14.12

The last three climatology values were based on the average timing of the peak wind in the verification data set and the Phase I and II developmental data sets. The average timing for the verification data set was 9.8 hours, while the Phase I and II data sets had an average timing of 9.7 hours. The MesoNAM forecasts for the timing of the peak wind were derived by determining when the peak wind occurred at model levels 2-18, as well as the strongest wind in the lowest 1000-, 2000- and 3000-ft of the model.

Figure 28 compares the mean error (diamonds) and MAE (circles) of the timing of the peak wind, in hours. The Phase I (point 1) method had a bias near zero. The Phase II methods using least-squares single linear regressions (points 1-6, in yellow) also had a bias near zero, while the robust single linear regressions (points 7-12, in yellow) had a large negative bias, around 4 hours. The 0000 UTC MesoNAM winds (points 1-20, in blue) had a positive bias around 2 hours. The first three climatology values had a negative bias of 4-5 hours, while the last three climatology values had a bias near zero. None of the methods performed significantly better than climatology.

Figure 29 compares the mean error (diamonds) and MAE (triangles) for the 0000 and 1200 UTC runs of the MesoNAM. There was little difference in MAE between the 0000 and 1200 UTC runs. All of the model winds had a positive bias, although the bias was larger in the 1200 UTC model runs. Since none of the methods improved significantly upon climatology, the 45 WS forecasters should use climatology for the timing of the peak wind until a more accurate method can be developed.

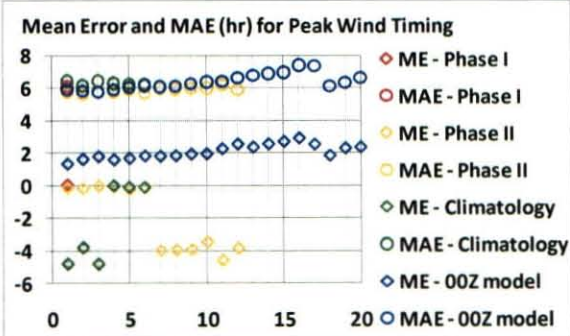


Figure 28. Mean Error (diamonds) and MAE (circles) for timing of the peak wind. The Phase I method is plotted on point 1, Phase II methods on points 1-12, climatology methods on points 1-4 and 0000 UTC MesoNAM winds on points 1-20.

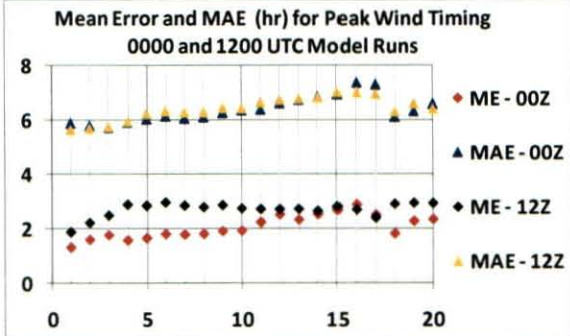


Figure 29. The Mean Error (diamonds) and MAE (triangles) for the timing of the peak wind by the 0000 and 1200 UTC MesoNAM winds.

## 5 Peak Wind Tool GUIs

The AMU delivered the Phase II tool as a Microsoft Excel GUI. The 45 WS also requested a tool for MIDDs, their main weather display system. The Excel and MIDDs tools display the same forecast parameters: PWSD, AWSD, and the probability the peak wind will meet or exceed 25 kt, 35 kt and 50 kt. Unlike Phase I, the Phase II tool does not display the timing of the peak wind since none of the methods improved upon climatology. The Excel GUI uses the 0000 and 1200 UTC MesoNAM winds as input, therefore it can display predictions for the Day-1 to Day-3 forecast periods. The MIDDs tool uses winds from the 0000 and 1200 UTC MesoNAM and Global Forecast System (GFS) models. The MIDDs tool can use the MesoNAM winds to display predictions for the Day-1 to Day-3 forecast periods, and use the GFS winds to display predictions for the Day-1 to Day-7 forecast periods.

### 5.1 Microsoft Excel GUI

The Phase I version of the Excel GUI used the morning XMR sounding as input to the prediction equations. The 45 WS forecaster manually entered sounding data, and then the GUI calculated and displayed the predicted PWSD, AWSD, timing of the PWSD and the probability the peak speed will meet or exceed 35 kt, 50 kt and 60 kt. The 45 WS no longer issues wind advisories for peak winds of 60 kt or greater, therefore, the Phase II version does not display the probability the peak speed will meet or exceed 60 kt. However, the 45 WS did request the AMU add the probability the peak speed will meet or exceed 25 kt, therefore the Phase II version displays the probability the peak speed will meet or exceed 25 kt, 35 kt and 50 kt. Since the MesoNAM linear regression forecasts performed the best for PWSD and AWSD in the verification, the Phase II version uses MesoNAM forecast winds as input. MesoNAM forecasts are provided to the 45 WS by ACTA, Inc. and include hourly forecasts from 0 to 84 hours based on the model runs at 0000, 0600, 1200 and 1800 UTC. The 45 WS receives the MesoNAM forecasts via e-mail after each model run, and they can be stored on a computer hard drive as a text file.

#### 5.1.1 Equation Development

The AMU created single linear regression equations for the Day-1 to Day-3 forecasts of PWSD and AWSD, using both the 0000 and 1200 UTC MesoNAM forecast winds. The equations were developed with MesoNAM forecasts from the same POR as the verification data set, March 2007 to April 2009. The data were first stratified by precipitation and non-precipitation days. Equations were then developed for each model level, from level 2 to level 18, as well as the lowest 1000-, 2000- and 3000-ft.

Figure 30 and Figure 31 show the MAE values for PWSD from the 0000 UTC and 1200 UTC MesoNAM regression forecasts, respectively. As expected, the Day-1 forecasts were the most accurate, followed by the Day-2 and Day-3 forecasts. The forecasts were significantly more accurate on non-precipitation days. On precipitation days, the 1200 UTC runs were more accurate than the 0000 UTC runs, especially for Day-3. On non-precipitation days, the forecasts from the 0000 and 1200 UTC runs were very similar.

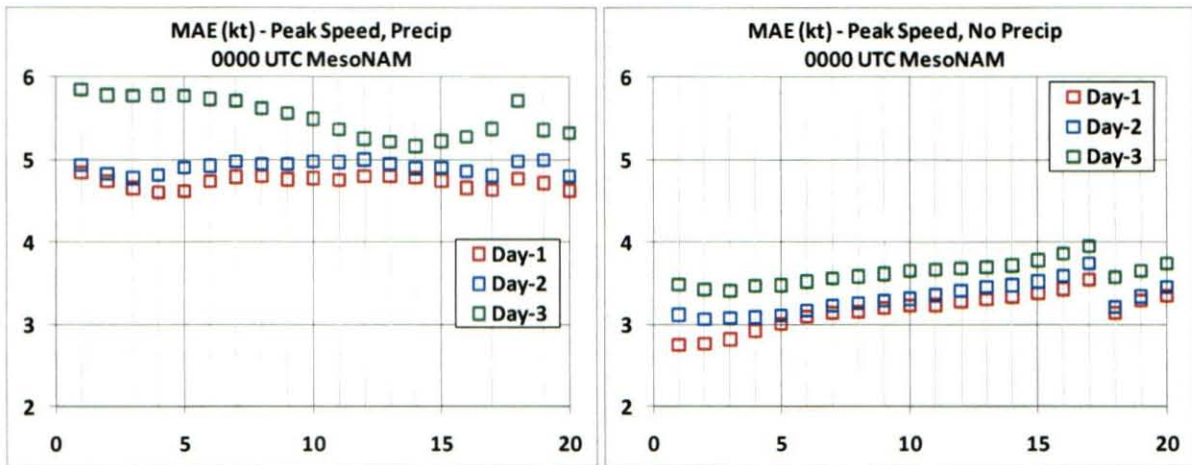


Figure 30. MAE for PWSD on precipitation (left) and non-precipitation (right) days, for Day-1 to Day-3 forecasts. Forecasts are from linear regression equations using the 0000 UTC MesoNAM forecast winds. Points 1-17 depict model levels 2-18, and points 18-20 depict the strongest winds in the lowest 1000-, 2000- and 3000-ft of the model.

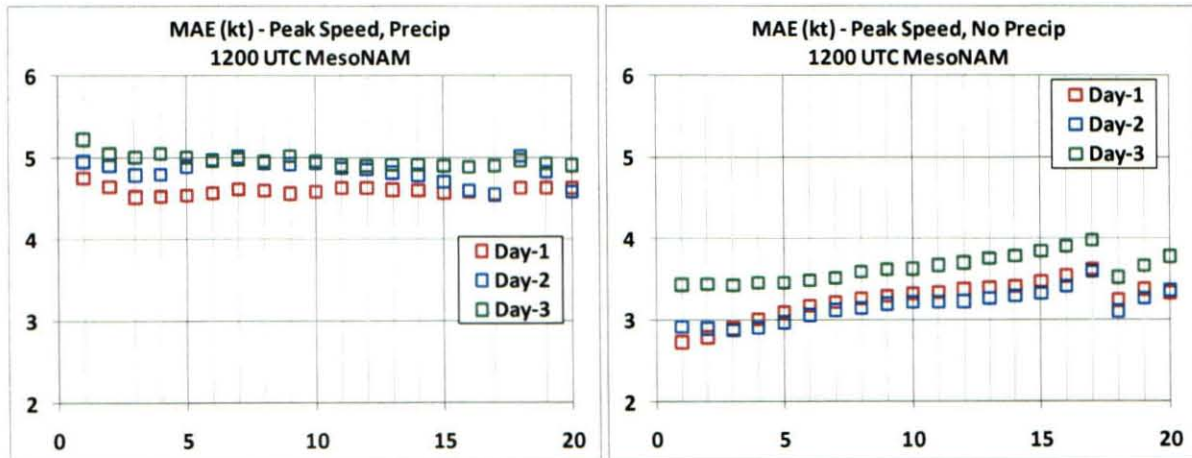


Figure 31. MAE for PWSD on precipitation (left) and non-precipitation (right) days, for Day-1 to Day-3 forecasts. Forecasts are from linear regression equations using the 1200 UTC MesoNAM forecast winds. Points 1-17 depict model levels 2-18, and points 18-20 depict the strongest winds in the lowest 1000-, 2000- and 3000-ft of the model.

Figure 32 and Figure 33 show the MAE values for AWS. The Day-1 and Day-2 forecasts had similar MAE values. The Day-3 forecasts were worse than the Day-1 and Day-2 forecasts, except the Day-2 and Day-3 forecasts from the 0000 UTC runs were similar on non-precipitation days. On precipitation days, the 1200 UTC forecasts were slightly more accurate than the 0000 UTC forecasts.

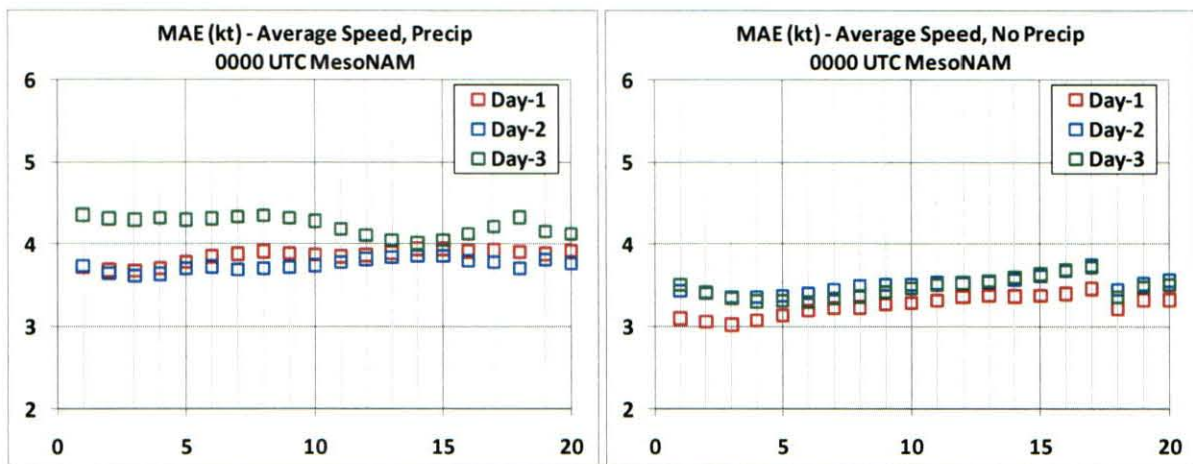


Figure 32. MAE for AWSD on precipitation (left) and non-precipitation (right) days, for Day-1 to Day-3 forecasts. Forecasts are from linear regression equations using the 0000 UTC MesoNAM forecast winds. Points 1-17 depict model levels 2-18, and points 18-20 depict the strongest winds in the lowest 1000-, 2000- and 3000-ft of the model.

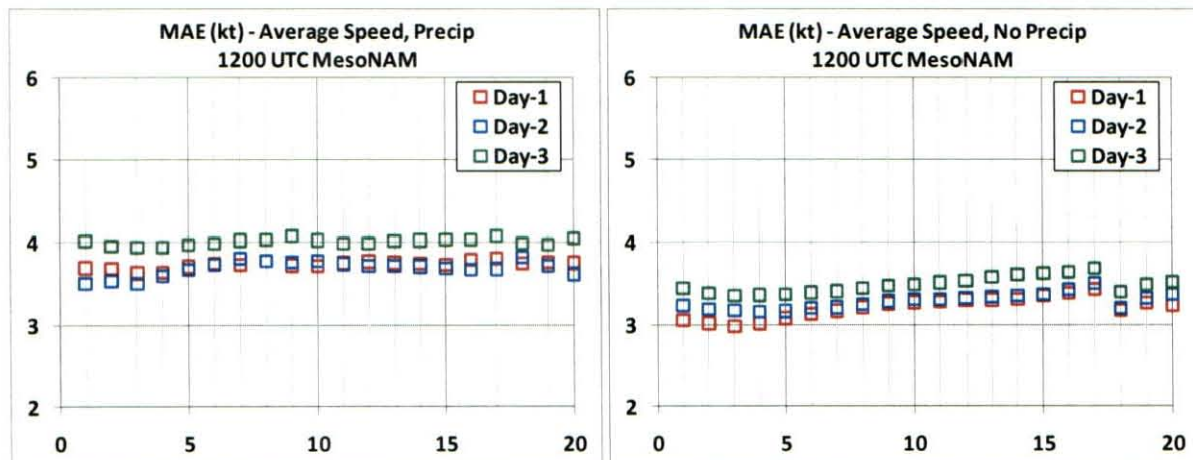


Figure 33. MAE for AWSD on precipitation (left) and non-precipitation (right) days, for Day-1 to Day-3 forecasts. Forecasts are from linear regression equations using the 1200 UTC MesoNAM forecast winds. Points 1-17 depict model levels 2-18, and points 18-20 depict the strongest winds in the lowest 1000-, 2000- and 3000-ft of the model.

For each forecast parameter, the tool uses the model level with the most accurate equation, based on the lowest MAE values. Since the tool uses separate equations for precipitation and non-precipitation days, as well as each forecast day, 12 prediction equations are used for both PWSD and AWSD. Table 10 and Table 11 describe the PWSD and AWSD equations used in the Excel GUI.

Table 10. Prediction equations for PWSD, based on linear regressions in which the predictor is the strongest 24-hour wind speed at the MesoNAM model level, and the predictand is the PWSD. Refer to Table 7 for the height of each model level.

<i>Forecast Day</i>	<i>Precipitation Occurrence</i>	<i>Model Run (UTC)</i>	<i>Model Level</i>	<i>MAE (kt)</i>	<i>Slope</i>	<i>Intercept</i>
Day-1	Yes	0000	5	4.61	1.05	7.99
Day-1	No	0000	2	2.76	1.08	5.55
Day-1	Yes	1200	4	4.53	1.10	7.87
Day-1	No	1200	2	2.73	1.13	5.41
Day-2	Yes	0000	4	4.78	1.08	8.76
Day-2	No	0000	3	3.07	0.98	6.72
Day-2	Yes	1200	18	4.56	0.58	16.24
Day-2	No	1200	4	2.88	0.99	5.84
Day-3	Yes	0000	15	5.17	0.58	17.04
Day-3	No	0000	3	3.42	0.95	7.54
Day-3	Yes	1200	17	4.89	0.65	14.45
Day-3	No	1200	4	3.43	0.90	7.60

Table 11. Prediction equations for AWSD, based on linear regressions in which the predictor is the strongest 24-hour wind speed at the MesoNAM model level, and the predictand is the AWSD. Refer to Table 7 for the height of each model level.

<i>Forecast Day</i>	<i>Precipitation Occurrence</i>	<i>Model Run</i>	<i>Model Level</i>	<i>MAE (kt)</i>	<i>Slope</i>	<i>Intercept</i>
Day-1	Yes	0000	4	3.68	0.78	4.76
Day-1	No	0000	4	3.02	0.75	2.25
Day-1	Yes	1200	4	3.64	0.81	4.31
Day-1	No	1200	4	2.98	0.76	2.59
Day-2	Yes	0000	4	3.61	0.79	4.76
Day-2	No	0000	5	3.36	0.63	4.20
Day-2	Yes	1200	2	3.51	0.82	5.37
Day-2	No	1200	5	3.16	0.67	3.53
Day-3	Yes	0000	15	4.01	0.40	11.62
Day-3	No	0000	5	3.30	0.64	4.28
Day-3	Yes	1200	5	3.94	0.71	5.91
Day-3	No	1200	4	3.36	0.66	4.17

In Phase I, the 45 WS developed a statistical method for estimating the probability the PWSD will meet or exceed the thresholds for wind advisories (Barrett and Short 2008). The method is based on the error bars of the linear regression equations. The equation for calculating the probabilities gives the area under the right-side of the Gaussian curve:

$$1 - \left[ 0.5 * \left( 1 \pm \sqrt{1 - e^{\left( -2 / \pi * \left( (x-y) / z \right)^2 \right)}} \right) \right]$$

In the equation, x is the threshold value (25, 35 and 50), y is the predicted PWSD and z is the predicted sigma (estimated error of the linear regression equation). The + sign before the radical is used for  $y \leq x$ , and the - sign is used for  $y > x$ .

### 5.1.2 Using the Excel GUI

The AMU developed the Excel GUI using the Visual Basic for Applications programming language. To use the tool, the forecaster opens the Excel file to the “Intro” worksheet (Figure 34). The Intro worksheet contains instructions on how to use the tool. Common user questions are answered in the “FAQs” (Frequently Asked Questions) worksheet. To start the tool, the forecaster selects the “Start Cool-Season Peak Wind Calculation” button. The tool then displays a “Browse” dialog box containing a list of files. The dialog box opens to the file directory last used. The forecaster needs to navigate to the directory containing the MesoNAM files and select one of the files (Figure 35).

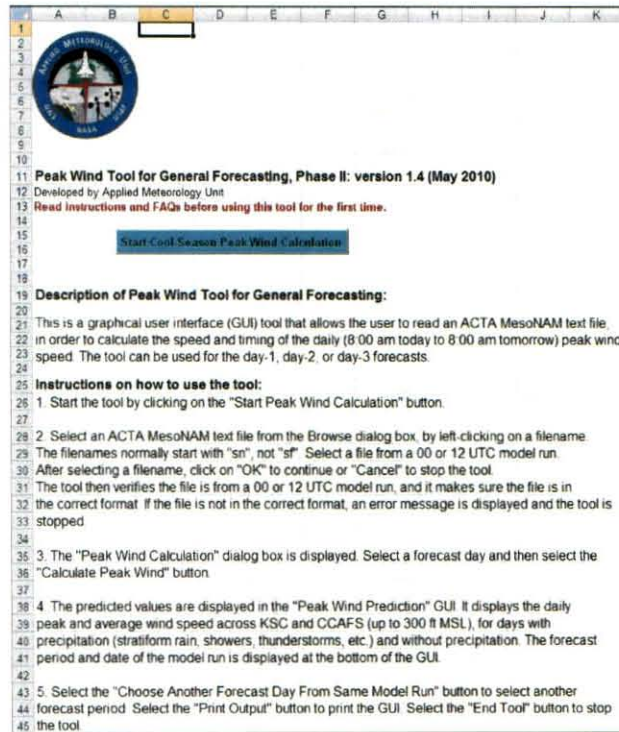


Figure 34. Intro worksheet to start the Excel version of the Peak Wind Tool.

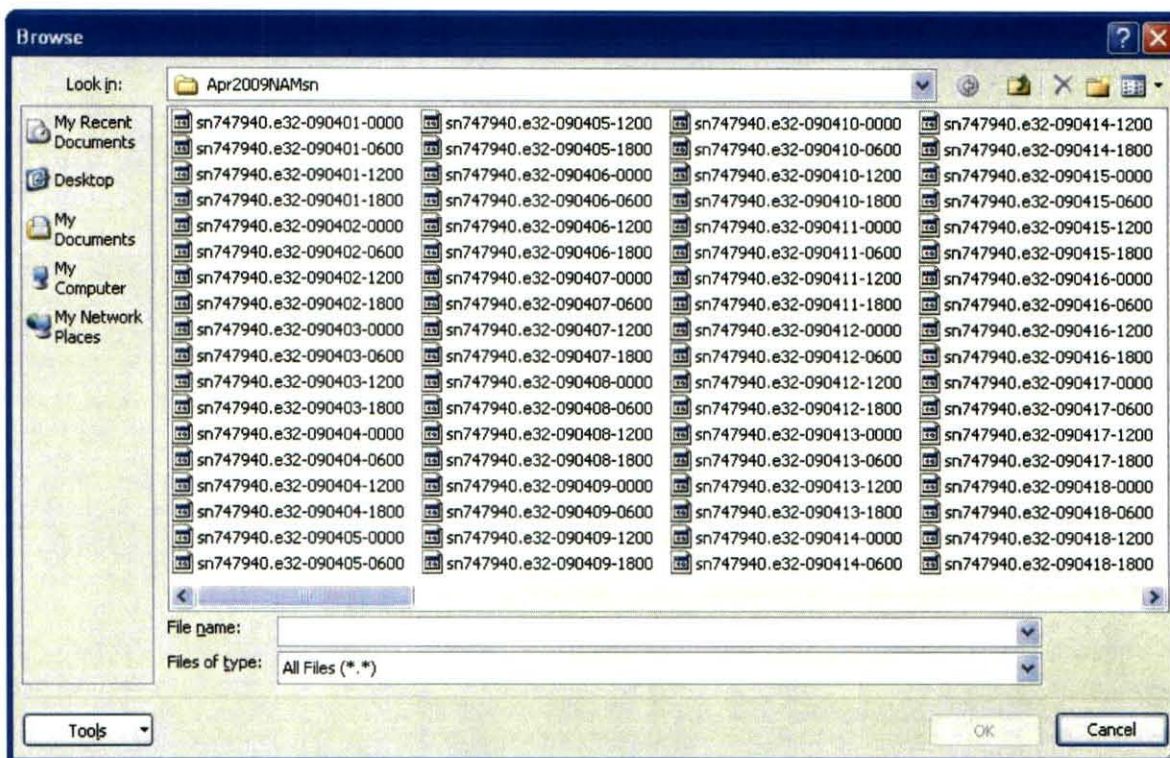


Figure 35. Dialog box used to select a MesoNAM input file.

The tool verifies the file chosen by the forecaster is in the correct format and is from a 0000 or 1200 UTC run of the MesoNAM. If the file is invalid, the tool displays an error message and exits. Otherwise, the “Peak Wind Calculation” dialog box is displayed (Figure 36). The dialog box shows the date and time of the model run. In this example, it is the 0000 UTC run from 1 April 2009. The forecaster selects a forecast day and then selects the “Calculate Peak Wind” button. The Peak Wind Prediction GUI with the desired output is then displayed (Figure 37). The GUI shows the forecasts for PWSD, AWSD and the probability the peak wind will meet or exceed 25 kt, 35 kt and 50 kt. The left/right side of the GUI shows the forecasts for precipitation days/non-precipitation days. Since no methods for predicting the timing of the PWSD performed better than climatology, the GUI contains the following note: “The peak wind speed of the day usually occurs during the afternoon or evening. The climatological timing of the peak speed is 2248 UTC. Adjust the time of the peak wind, based on expected movement of fronts, wind surges, changes in pressure gradient, etc.” The forecast period is displayed at the bottom of the GUI. In this example, the forecast period is from 1 April 2009 (0800 local) to 2 April 2009 (0800 local). The forecaster can then select one of three options: “Print Output”, “Choose Another Forecast Day From Same Model Run” and “End Tool”.

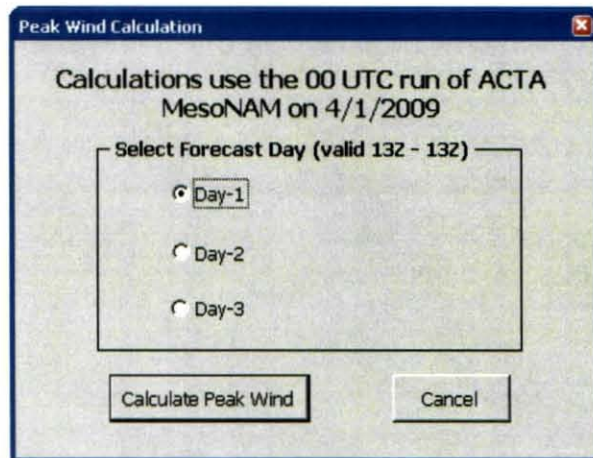


Figure 36. Dialog box used to select the forecast day.

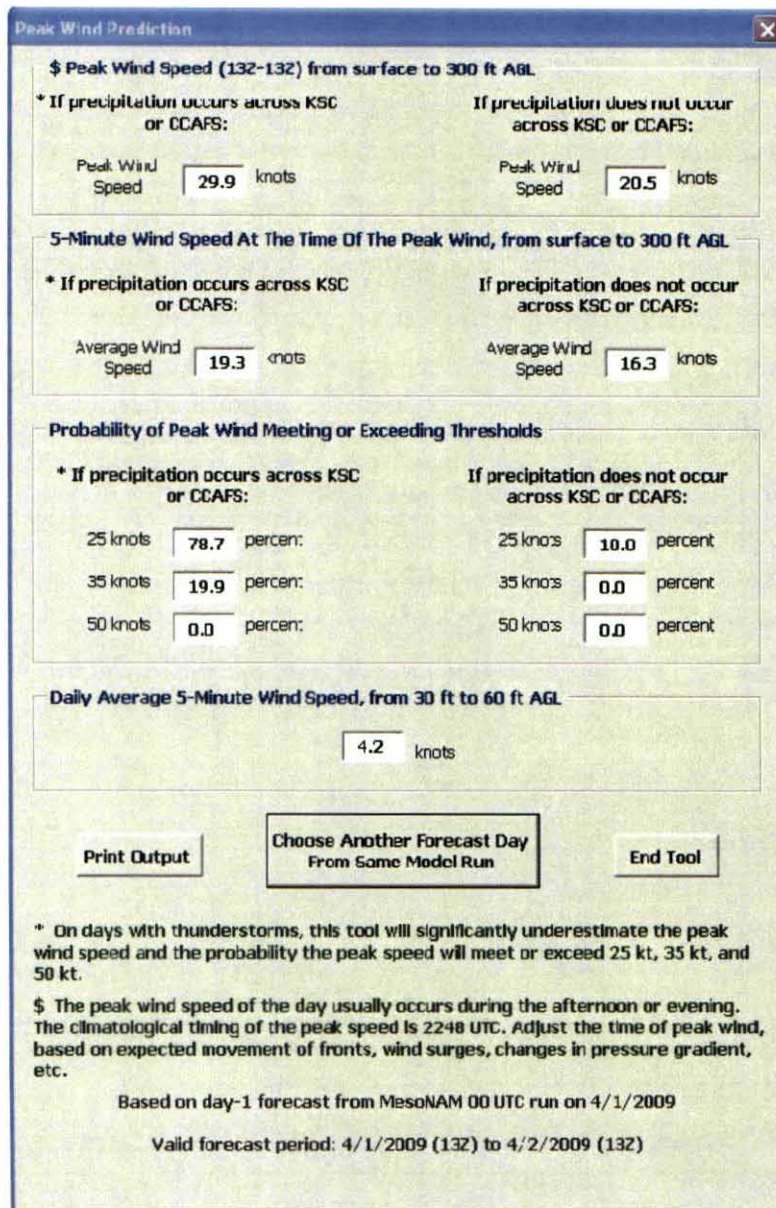


Figure 37. GUI displaying the output from the Excel version of the Peak Wind tool. The top section shows the predicted PWSD, the middle section shows the predicted AWSD, and the bottom section shows the probability the PWSD will meet or exceed 25 kt, 35 kt and 50 kt.

## 5.2 MIDDs GUI

The AMU initially developed the MIDDs tool to use gridded model data as input because the ACTA MesoNAM files are not available in MIDDs. The tool was created using the Tool Command Language/Tool Kit (Tcl/Tk) programming language. It used the model data for the closest grid point to XMR. The MIDDs gridded data contains output from the 0000 and 1200 UTC model runs of the North American Mesoscale (NAM) and GFS models. Both models have a horizontal grid spacing of 80 km in

MIDDS. After the 45 WS was given access to receive point model data from Johnson Space Center, the tool was modified to use these data.

### **5.2.1 Equation Development**

While the MesoNAM contains hourly forecasts out to 84 hours, the NAM and GFS gridded data in MIDDS contain 6-hourly forecasts out to 60 hours and 240 hours, respectively. The MIDDS tool used NAM data to generate Day-1 and Day-2 forecasts and GFS data to generate Day-1 to Day-5 forecasts. The Day-1, Day-2 and Day-3 forecast equations developed for the Excel tool were also used for the Day-1, 2 and 3 forecasts in the MIDDS tool. The Day-3 forecast equations were used for the Day-4 and Day-5 forecasts. The forecasts based on the GFS gridded model data used the MesoNAM linear regression equations developed for the Excel tool, since the verification data set did not contain GFS model data.

Since the MIDDS gridded model forecasts are only available every six hours, the AMU updated the linear regression equations to take the forecast interval into account. Otherwise, the MIDDS tool would have a low bias in predicting wind speeds. The MIDDS tool calculates the probability the PWSD will meet or exceed 25 kt, 35 kt and 50 kt, using the same statistical method as the Excel tool (Section 5.1.1).

Based on feedback from the 45 WS, least-squares single linear regression equations were developed for the daily average wind speed at 30-60 ft, which is one of the forecast parameters in the 24-Hour and Weekly Planning Forecasts issued by the 45 WS. The predictands were calculated by averaging the 5-minute average wind speeds at 30 ft and 54/60 ft from all of the towers used in this task through a 24-hour period (1300 UTC to 1300 UTC). The predictors were calculated by averaging the hourly MesoNAM winds for the 24-hour period. The predictors were evaluated for model levels 1 and 2 of the MesoNAM, which have average heights of 70 ft and 207 ft MSL, respectively.

Figure 38 shows the MAE for daily average wind speed from the 0000 (left) and 1200 UTC (right) model runs. The level-1 (in blue) and level-2 (in red) forecasts are compared to climatology (in green) for Day-1 to Day-3, including precipitation days, non-precipitation days and “all days”. The “all days” forecasts included precipitation and non-precipitation days. Separate climatology values were calculated for precipitation days (8.4 kt), non-precipitation days (6.8 kt) and “all days” (7.3 kt). The level-2 forecasts performed slightly better than level-1 forecasts and significantly better than climatology. As expected, the MAE values were lowest on non-precipitation days and highest on precipitation days. The MAE values increased slightly from Day-1 to Day-3. There was not much difference between the 0000 and 1200 UTC runs, except the level-1 and level-2 forecasts from the 1200 UTC runs did better than the 0000 UTC runs for Day-3.

The forecasts for “all days” were then compared to the average of the precipitation and non-precipitation days, weighted by the number of precipitation and non-precipitation days. Table 12 shows the differences between the “all days” forecasts and weighted average forecasts were not significant. Therefore, unlike for PWSD and AWS, the prediction equations for daily average wind speed did not stratify by precipitation.

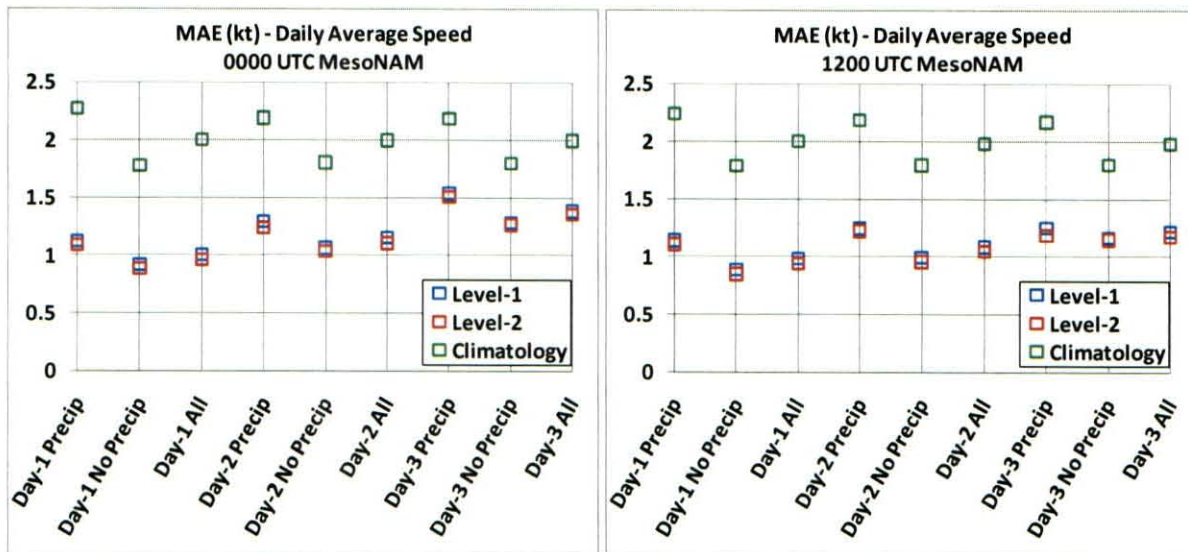


Figure 38. MAE for daily average speed for forecasts from 0000 (left) and 1200 UTC (right) MesoNAM. Forecasts for precipitation days are plotted on points 1, 4 and 7 of the x-axis. Forecasts for non-precipitation days are plotted on points 2, 5 and 8, and forecasts for all days are plotted on points 3, 6 and 9.

Table 12. MAE (kt) for daily average speed. “All Days” is all days in the verification data set. “W. Avg” is the weighted average of precipitation and non-precipitation days. “00 UTC” is the 0000 UTC MesoNAM and “12 UTC” is the 1200 UTC MesoNAM.

Forecast Day	Level-1 00 UTC All Days	Level-1 00 UTC W. Avg	Level-2 00 UTC All Days	Level-2 00 UTC W. Avg	Level-1 12 UTC All Days	Level-1 12 UTC W. Avg	Level-2 12 UTC All Days	Level-2 12 UTC W. Avg
Day-1	1.00	0.99	0.96	0.95	0.98	0.97	0.94	0.93
Day-2	1.15	1.14	1.11	1.10	1.08	1.07	1.05	1.04
Day-3	1.39	1.37	1.36	1.34	1.22	1.19	1.17	1.16

### 5.2.2 Point Model Data

The 45 WS MIDDS workstations were given access to point model data from a MIDDS server at Johnson Space Center. The MIDDS point model data are available for the MesoNAM and GFS models. The MIDDS point model data have a higher vertical resolution than the gridded model data. For example, the vertical levels in the gridded model data are primarily confined to the NWS mandatory sounding levels (surface, 1000 mb, 925 mb, 850 mb, etc.). On the other hand, the point model data include all of the model’s vertical levels. The MesoNAM contains 60 vertical levels from the surface to 14.5 mb, while the GFS model contains 64 vertical levels from the surface to 0.29 mb. The point model data also have a higher temporal resolution. While MIDDS gridded model forecasts are available every six hours, point model forecasts are available every three hours from the GFS and every hour from the MesoNAM. In order to increase the accuracy of the tool, the AMU updated the tool to use the higher resolution point model data. The tool’s source code and installation instructions were then delivered to the 45 WS for operational use.

### 5.2.3 Using the MIDDS GUI

To use the MIDDS tool, the forecaster first opens it from the MIDDS Weather Menu. The tool reads in MesoNAM and GFS data from the latest 0000 and 1200 UTC model runs. After the tool has finished reading the model data, it displays the message “Initialization Complete”. The user selects a model name

(NAM or GFS) and model run (“00Z” or “12Z”) and then selects the “Calculate Peak Wind” button. The tool calculates and displays the forecasts for PWSD, AWSD, daily average wind speed, and the probability the peak wind will meet or exceed 25 kt, 35 kt and 50 kt. Except for the daily average wind speed, separate forecasts are made for days with and without precipitation. Based on feedback from the 45 WS, the tool was updated to provide forecasts out to Day-7. Therefore, the MesoNAM forecasts are for Day-1 to Day-3, while the GFS forecasts are for Day-1 to Day-7. Figure 39 shows the tool’s forecasts from the model runs on 7 July 2010. The forecaster has the option of printing out the displayed forecasts by selecting the “Print Display” button. The user closes the tool by selecting the “Exit Tool” button.

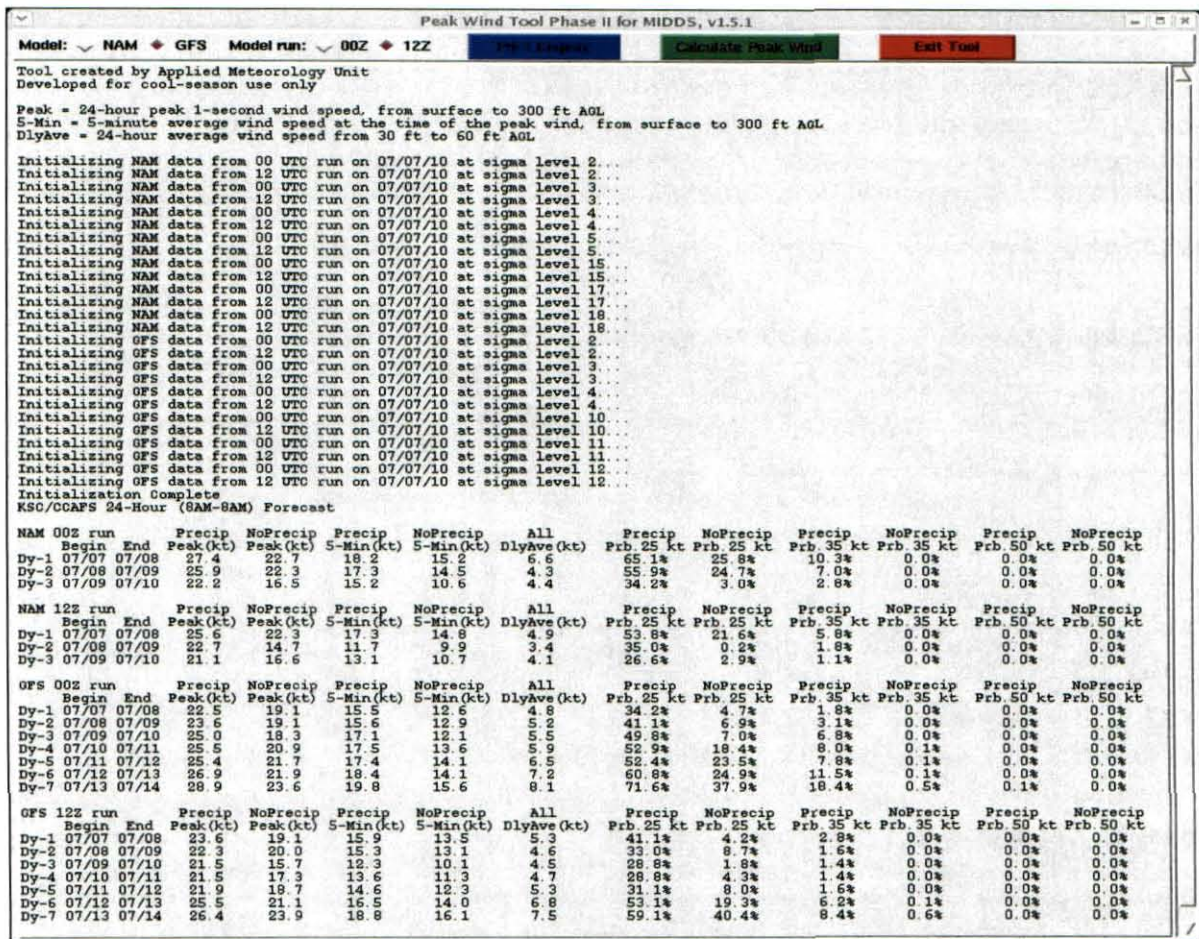


Figure 39. MIDDs version of the Peak Wind Tool showing forecasts from the 7 July 2010 model runs. Forecasts for precipitation days have the header “Precip”, while non-precipitation days have the header “NoPrecip”. The header “All” includes days with and without precipitation.

## 6 Summary and Future Work

The expected peak wind speed is an important element in the 45 WS daily 24-Hour and Weekly Planning Forecasts. The forecasts are used for ground and space launch operations at KSC and CCAFS. The 45 WS forecasters have indicated peak wind speeds are challenging to forecast, especially in the cool season months of October - April. In Phase I of this task (Barrett and Short 2008), the AMU developed a Microsoft Excel tool to help the 45 WS forecast non-convective winds at KSC/CCAFS for the 24-hour period of 0800 to 0800 local time. The tool displayed forecasts for the PWSD, AWSD, timing of the PWSD and the probability the PWSD will meet or exceed the 45 WS wind advisory thresholds of 35 kt, 50 kt and 60 kt. The wind advisory threshold for 60 kt wind gusts was later dropped and a threshold for 25 kt added. For Phase II, the 45 WS requested the AMU expand the POR to increase the number of observations used in the creation of the prediction equations. In addition to an Excel tool, the 45 WS also requested a MIDDs tool to provide forecasts out to seven days.

### 6.1 Summary

The AMU first expanded the POR by two years, by adding KSC/CCAFS tower observations, SLF surface observations and XMR soundings for the cool season months of March 2007 to April 2009. The prediction equations required sounding data in 100-ft increments. The AMU evaluated whether the POR could be expanded even more by interpolating 1000-ft sounding data down to 100-ft increments. A comparison showed no significant differences between the interpolated and 100-ft sounding data. Therefore, the POR was expanded again by six years after adding interpolated sounding data for the cool season months of October 1996 to April 2002.

The Phase II developmental data set contained tower observations, surface observations and soundings for the cool season months of October 1996 to February 2007. The AMU calculated candidate predictors from the XMR soundings. The predictors included 19 stability parameters, 48 wind speed parameters and one wind shear parameter. The data set was stratified by synoptic weather pattern, low-level wind direction, precipitation, Richardson Number and Gradient Richardson Number, for a total of 60 stratification methods. Linear regression equations, using the 68 predictors and 60 stratification methods, were created for the tool's three forecast parameters (PWSD, AWSD, and timing of the PWSD). Instead of selecting the most accurate Phase II method for each forecast parameter, several well-performing methods were selected for evaluation in the verification data set.

The verification data set contained observations for the cool season months of March 2007 to April 2009. The verification data set was used to compare the Phase I and II prediction methods to climatology, model forecasts and wind advisories issued by the 45 WS. The comparison was first performed for PWSD and AWSD. The Phase II methods performed slightly better than Phase I and significantly better than climatology. The Phase I and II methods were then compared to the 0000 and 1200 UTC runs of the MesoNAM. The MesoNAM data contained wind forecasts for model levels 2 - 18 (between 207 ft and 3145 ft MSL), as well as the strongest winds in the lowest 1000-, 2000- and 3000-ft of the model. Linear regression equations were created, in which the predictor was the 24-hour peak speed in the MesoNAM data and the predictand was the PWSD or AWSD. The MesoNAM linear regression equations performed significantly better than the Phase I and II methods. The Phase I and II forecasts of PWSD were compared to wind advisories issued by the 45 WS. On days in which the 45 WS issued at least one non-convective wind advisory, the 45 WS out-performed the Phase I and II methods.

The verification data set was then used to evaluate the Phase I and II methods for the timing of the PWSD. The Phase I and II methods were compared to climatological winds and the 0000 and 1200 UTC runs of the MesoNAM. The MesoNAM forecasts were derived by determining when the 24-hour peak wind occurred at each model level. The Phase I and II methods, as well as the MesoNAM forecasts, did not perform significantly better than climatology.

The Microsoft Excel and MIDDS versions of the tool were then developed by the AMU. The tool displays forecasts for the PWSD, AWSD and the probability the PWSD will meet or exceed 25 kt, 35 kt and 50 kt. The probabilities, based on the PWSD, were calculated using a statistical method developed by the 45 WS (Barrett and Short 2008). For PWSD and AWSD, the tool uses linear regression equations based on the 0000 and 1200 UTC MesoNAM forecast winds. Since none of the prediction methods for the timing of the peak wind performed significantly better than climatology, the tool does not provide forecasts for the timing of the peak wind. Instead, the forecaster should use climatology to forecast the timing of the peak wind. The forecaster can then adjust the timing based on the movement of weather features. The Excel and MIDDS GUIs display forecasts for Day-1 to Day-3 and Day-1 to Day-7, respectively. The Excel GUI uses MesoNAM point forecasts as input, while the MIDDS GUI uses point forecasts from the MesoNAM and GFS models. The AMU also updated the Microsoft Excel and MIDDS tools to provide the daily average wind speed from 30 ft to 60 ft AGL, which is one of the forecast parameters in the 24-Hour and Weekly Planning Forecasts issued by the 45 WS.

## **6.2 Future Work**

The 45 WS proposed a follow-on task (Phase III) to the Peak Wind tool. Instead of providing 24-hour forecasts from Day-1 to Day-7, the Phase III tool would display 4-hour forecasts for Day-1, then 12-hour forecasts for Day-2 to Day-7. The Phase III tool would not provide forecasts for AWSD or timing of the PWSD. Instead, the tool would provide forecasts for PWSD, daily average wind speed and the probability the PWSD will meet or exceed 25 kt, 35 kt and 50 kt. Phase III would also expand the POR for the MesoNAM forecasts to October 2006 to April 2010.

## References

- Barrett, J. H. and D. A. Short, 2008: Peak Wind Tool for General Forecasting Final Report. NASA Contractor Report CR-2008-214743, Kennedy Space Center, FL, 59 pp. [Available from ENSCO, Inc., 1980 N. Atlantic Ave., Suite 230, Cocoa Beach, FL 32931 and <http://science.ksc.nasa.gov/amu/final.html>]
- Case, J. L. and W. H. Bauman III, 2004: Tower Mesonetwork Climatology and Interactive Display Tool Final Report. NASA Contractor Report CR-2004-211526, Kennedy Space Center, FL, 80 pp. [Available from ENSCO, Inc., 1980 N. Atlantic Ave., Suite 230, Cocoa Beach, FL 32931 and <http://science.ksc.nasa.gov/amu/final.html>]
- Insightful, 2002: S-PLUS 6 Robust Library User's Guide, Insightful Corporation, Seattle, WA, 188 pp.
- Insightful, 2007: S-PLUS 8 Guide to Statistics, Volume 1, Insightful Corporation, Seattle, WA, 718 pp.
- Lambert, W. C., 2002: Statistical Short-Range Guidance for Peak Wind Speed Forecasts on Kennedy Space Center/Cape Canaveral Air Force Station: Phase I Results Final Report. NASA Contractor Report CR-2002-211180, Kennedy Space Center, FL, 33 pp. [Available from ENSCO, Inc., 1980 N. Atlantic Ave., Suite 230, Cocoa Beach, FL 32931 and <http://science.ksc.nasa.gov/amu/final.html>]

### List of Acronyms

<b>Term</b>	<b>Description</b>
45 WS	45th Weather Squadron
AGL	Above Ground Level
AMU	Applied Meteorology Unit
AWSD	5-minute average wind speed at the time of the PWSD
CCAFS	Cape Canaveral Air Force Station
CSR	Computer Sciences Raytheon
EST	Eastern Standard Time
FAQ	Frequently Asked Questions
GFS	Global Forecast System
GUI	Graphical User Interface
KSC	Kennedy Space Center
MAE	Mean Absolute Error
MesoNAM	12-km North American Mesoscale Model
MIDDS	Meteorological Interactive Data Display System
MSL	Mean Sea Level
NAM	40-km or 80-km North American Mesoscale Model
NWS	National Weather Service
PAFB	Patrick Air Force Base
POR	Period Of Record
PWSD	Peak Wind Speed of the Day
QC	Quality Control
SLF	Shuttle Landing Facility
Tcl/Tk	Tool Command Language/Tool Kit
XMR	CCAFS rawinsonde 3-letter identifier

**NOTICE**

Mention of a copyrighted, trademarked or proprietary product, service, or document does not constitute endorsement thereof by the author, ENSCO Inc., the AMU, the National Aeronautics and Space Administration, or the United States Government. Any such mention is solely for the purpose of fully informing the reader of the resources used to conduct the work reported herein.